1 **Title: Projecting species distributions using fishery-dependent data**

2 **Running title:** Fishery-dependent SDM projections

3 **Authors**: Melissa A. Karp[1]*^, Stephanie Brodie[2,3], James A. Smith[3,4], Kate Richerson[5], Rebecca
4 L. Selden[6], Owen Liu[5], Barbara Muhling[3,4], Jameal F. Samhouri[5], Lewis A.K. Barnett[7], Elliott
5 Hazen[2], Daniel Ovando[8], Jerome Fiechter[9], Michael G. Jacox[2,3,10], Mercedes Pozo Buil[2,3]

6 [1] ECS Tech, *in support of*, Office of Science & Technology, National Marine Fisheries Service,
7 National Oceanic and Atmospheric Administration, Silver Spring, MD, USA
8 [2] Environmental Research Division, Southwest Fisheries Science Center, National Marine
9 Fisheries Service, National Oceanic and Atmospheric Administration, Monterey, CA, USA
10 [3] Institute of Marine Sciences, University of California Santa Cruz, Monterey, CA, USA
11 [4] Fisheries Resources Division, Southwest Fisheries Science Center, National Marine Fisheries
12 Service, National Oceanic and Atmospheric Administration, La Jolla, CA, USA
13 [5] Northwest Fisheries Science Center, National Marine Fisheries Service, National Oceanic and
14 Atmospheric Administration, Seattle, WA, USA 98112
15 [6] Department of Biological Sciences, Wellesley College, Wellesley, MA, USA
16 [7] Alaska Fisheries Science Center, National Marine Fisheries Service, National Oceanic and
17 Atmospheric Administration, Seattle, WA, USA
18 [8]School of Aquatic and Fishery Sciences, University of Washington, Seattle, Washington, USA
19 [9]Ocean Sciences Department, University of California at Santa Cruz, Santa Cruz, CA, USA
20 [10] Physical Sciences Laboratory, Oceanic and Atmospheric Research, National Oceanic and
21 Atmospheric Administration, Boulder, CO, USA
22
23 ***Correspondence**
24 Melissa A. Karp
25 Office of Science & Technology, National Marine Fisheries Service, National Oceanic and
26 Atmospheric Administration, 1315 East West Highway, Silver Spring, MD
27 Email: melissa.karp@noaa.gov
28

^ current affiliation: Office of Science & Technology, National Marine Fisheries Service, National Oceanic and Atmospheric Administration, Silver Spring, MD

ABSTRACT

Many marine species are shifting their distributions in response to changing ocean conditions, posing significant challenges and risks for fisheries management. Species distribution models (SDMs) are used to project future species distributions in the face of a changing climate. Information to fit SDMs generally comes from two main sources: fishery-independent (scientific surveys) and fishery-dependent (commercial catch) data. A concern with fishery-dependent data is that fishing locations are not independent of the underlying species abundance, potentially biasing predictions of species distributions. However, resources for fishery-independent surveys are increasingly limited, therefore, it is critical we understand the strengths and limitations of SDMs developed from fishery-dependent data. We used a simulation approach to evaluate the potential for fishery-dependent data to inform SDMs and abundance estimates, and quantify the bias resulting from different fishery-dependent sampling scenarios in the California Current System (CCS). We then evaluated the ability of the SDMs to project changes in the spatial distribution of species over time, and compare the time-scale over which model performance degrades between the different sampling scenarios and as a function of climate bias and novelty. Our results show that data generated from fishery-dependent sampling can still result in SDMs with high predictive skill several decades into the future, given specific forms of preferential sampling which result in low climate bias and novelty. Therefore, fishery-dependent data may be able to supplement information from surveys that are reduced or eliminated for budgetary reasons to project species distributions into the future.

KEY WORDS: climate bias, climate change, extrapolation, novelty, species distribution models, virtual species

Table of Contents

INTRODUCTION

The world's climate is changing at an unprecedented rate. Over the last century global average temperature has increased by 0.85°C, resulting in biological responses across terrestrial, freshwater, and marine environments (Nye et al. 2009, Cheung et al. 2015, Morley et al. 2018, Pecl et al. 2017). Species may respond to a changing climate in a variety of ways, including acclimatizing, adapting, moving to an area with a more suitable environment, or even dying. The responses of species to climate change, such as the rate of change in distributions, are more pronounced in the ocean, which absorbs the majority of the excess atmospheric heat from greenhouse gas emissions (Sorte et al. 2010; Poloczanska et al. 2013, 2016; Pinsky et al 2019). Changes in species distributions pose significant challenges and risks to resource management and the communities and economies that depend on marine resources (Pinsky et al. 2019). This is particularly so for fisheries that are faced with species shifting outside of historical fishing areas or across management boundaries (Ishimura et al. 2013, Sumaila et al. 2020). In light of this, there is an increasing need to predict how marine species distributions will respond to changing conditions. Accurate projections of future species distributions can inform our understanding of potential impacts on fisheries and fishing communities, climate change risk assessments, and sustainable fisheries management that can anticipate, prepare and account for these changes (Rogers et al 2019, Selden et al 2019, Smith et al. 2021a).

Correlative species distribution models (SDMs) are increasingly being used to project future species distributions to aid management decision making in the face of a changing climate (Cheung et al. 2009; Hazen et al. 2013). SDMs use statistical methods to relate species

occurrence or abundance to underlying environmental conditions, and then use those fitted relationships to predict current and future distribution patterns (Elith et al. 2009; Guisan and Thuiller 2005). SDMs generally perform better when predicting within the same time and space as the data used for calibration (e.g. interpolation), but performance can decline when projecting into novel environmental conditions and locations (i.e. extrapolation) (Muhling et al. 2020; Meyer and Pebesma 2021). However, in some cases, SDMs can perform well when predicting abundance and distribution under novel conditions (Becker et al. 2019). As climate change continues to cause novel conditions to emerge (Smith et al. 2022), understanding when models can perform well and what factors impact SDM performance under novel conditions is increasingly important.

An important factor that can effect SDM performance, particularly with regard to their ability to accurately project species distributions far into the future, is quality of the training data used to fit the models. In the case of marine fisheries, occurrence and abundance data mainly come from two sources, fishery-independent and/or fishery-dependent data. Fishery-independent data are often collected through expensive research programs which conduct standardized scientific surveys over large areas. Fishery-independent data collected via scientifically designed and standardized sampling gear and designs are particularly valuable as these sampling properties facilitate straightforward empirical estimation of population density and abundance. However, due to high cost and logistical challenges, fishery-independent data may not be available for all species, seasons, and regions (Dennis et al. 2015). This is particularly the case for many highly migratory species, which tend to have large and dynamic ranges (Lynch et al. 2018).

Fishery-dependent data often come from scientific observers on commercial fishing vessels, fish tickets (i.e. landing receipts), and/or industry-reported logbooks, and are frequently the only distribution data available for many species. They may provide some advantages over fishery-independent data, particularly with respect to the number of observations available. Additionally, fishery dependent data may actually be preferred in certain circumstances. For example, when the goal is to understand how a species may interact with the fishery (Crear et al. 2021). However, a potential concern with fishery-dependent data is their non-probabilistic, preferential sampling scheme. Economic, social, and management factors drive the distribution

of fishing locations; for example, fishers actively seek out areas with expected high concentrations of their target species (Pennino et al. 2019), but also may make decisions on where to fish based on local knowledge and experience (St. Martin and Hall-Aber 2008), management restrictions such as bycatch avoidance, closed areas, and landings requirements, as well as economic considerations such as fuel costs influencing the distance they are able or willing to travel from ports (Wilen 2004; Smith and Wilen 2003; Daw 2008; Bucaram et al. 2013).

The locations of fishing activity are therefore not random, and not independent of the response variable (e.g. species abundance) (Diggle et al. 2010; Conn et al. 2017; Pennino et al. 2019). Such preferential sampling violates a statistical assumption that sampling locations have been chosen independently of the value expected at a given location, and can result in biased predictions of abundance and distribution (Diggle et al. 2010; Conn et al. 2017; Pennino et al. 2019; Rufener et al. 2021, Alglave et al. 2022). Additionally, the non-random nature of fishing locations often results in the fishery-dependent data being spatially clustered relative to the underlying spatiotemporal distribution of the target species, which can result in poor representation within the data of the complete range of environmental conditions present in an area (Kadmon et al. 2004). The quality of an SDM and its ability to provide accurate predictions, particularly under novel conditions, can be strongly affected by such spatially and environmentally biased sampling schemes (Kadmon et al. 2004; Stoa et al. 2018; Yates et al. 2018; Baker et al. 2022).

Despite a general understanding of these potential biases and impacts on SDM performance, more work is needed in assessing the relative magnitude of such biases coming from different types of fishery-dependent sampling and understanding the factors that impact the relative magnitude. Several recent studies show that fishery-dependent data does not always result in biased predictions and may still be appropriate to analyze with standard statistical approaches (Pennino et al. 2016; Ducharme-Barth et al. 2022), or can be complementary to fishery-independent data using integrated methods (Rufener et al. 2021, Alglave et al. 2022). Therefore, considering that resources are increasingly limited at agencies for fishery-independent surveys, it is critical we understand the strengths and limitations of SDMs developed for evaluating future fish distributions from fishery-dependent data.

In this study, we explore the potential for fishery-dependent data to inform SDMs and abundance estimates, and quantify the bias resulting from different fishery-dependent sampling scenarios in the California Current System (CCS; Fig. 1). Specifically, we ask:

1. How do various types of fishery-dependent sampling affect SDM performance, relative to a randomized sampling process?
2. What is the timescale over which future SDM performance degrades, and is it affected by the type of fishery-dependent sampling?

We use a simulation approach to generate the 'true' distribution of a species based on static relationships between abundance and environmental variables. We then simulate a random sampling and several different fishery-dependent sampling processes to collect species observations and fit two types of SDMs (generalized additive models (GAMs) and Boosted Regression Trees (BRTs)) to those data. We then evaluate the ability of the SDMs to project changes in abundance, center of gravity, and spatial patterns of distribution into the future, and compare the time-scale over which model performance degrades between the different sampling scenarios and as a function of climate bias and novelty. This simulation approach is advantageous because it allows us to test the impacts of different sampling scenarios on model performance against a known 'truth', which is not possible with *in situ* data.

METHODS

General Framework

To quantify the impact of fishery-dependent sampling bias on the ability of SDMs to predict current and project future species distributions, we used a simulation-estimation process consisting of four main steps (Fig. 2): 1) develop an operating model (OM) to simulate a virtual species distribution, 2) sample the virtual species distribution with simulated random and fishery-dependent sampling procedures, 3) use the simulated data (training period 1985-2010) to fit an estimation model (the SDM), and project the SDM from 2011 to 2100 under climate change, and 4) evaluate performance of fitted models by comparing the output of SDM predictions against the 'true' simulated observations. Here we provide an overview of the key aspects of the simulation. More details can be found in the Supplemental Methods and in Table

S1, and the Rcode for this simulation can be found on github (https://github.com/Melissa-Karp/Fishery-dependent-SDM-projections).

Operating model

We used the *virtualspecies* package (Leroy et al. 2016) in R version 3.6.1 (R Core Team 2019) to build our operating model. This enables us to not only simulate species-environment responses and convert habitat suitability to presence-absences or abundance, but also incorporate biases into the process of sampling occurrences.

Environmental variables

Environmental data were obtained from a California Current System (CCS) configuration of the Regional Ocean Modeling System (ROMS). This configuration covers 30-48˚N and inshore of 134˚W, with 0.1 degree (7-11 km) horizontal resolution and 42 terrain-following vertical levels (Veneziani *et al.* 2009, Pozo Buil *et al.* 2021). For projections of ocean conditions, the CCS ROMS model was forced by output for 1980-2100 from a global Earth System Model (ESM; HadGEM2-ES) under the RCP8.5 emission scenario. For this study, 1985-2010 was considered the 'historical' period, and 2011-2100 the 'future' period, but both periods were sourced from the same ESM-forced projection. To correct for biases in the ESM used to force ROMS, a "time-varying delta" method was applied before performing the downscaling with ROMS, in which ESM changes (calculated as departures from the 1980-2010 climatology) were added to the observed 1980-2010 climatology (Pozo Buil *et al.* 2021, Smith *et al.* 2021a). To project regional biogeochemical change (including phytoplankton biomass), ROMS is coupled to the biogeochemical model NEMUCSC (Fiechter *et al.* 2014; Fiechter *et al.* 2018) – an adapted version of the North Pacific Ecosystem Model for Understanding Regional Oceanography (NEMURO; Kishi *et al.* 2007). NEMUCSC consists of three limiting macronutrients, two phytoplankton size-classes, three zooplankton size-classes, and three detritus pools. Following the approach in Fiechter *et al.* (2018), NEMUCSC was coupled offline to the ROMS downscaled projection (Pozo Buil *et al.*, 2021). Environmental variables of interest were sea surface temperature (SST; C), mixed layer depth (MLD; m), surface chlorophyll-a (Chl-a; mg m-3), and zooplankton integrated over 200 m (zoo_200; mmol N m-2).

We used only one ESM to keep the simulation manageable, and selected HadGEM2-ES because it is at the upper end of projected end-of-century warming for the CMIP5 ensemble (~4˚C), and thus maximizes the signal to noise ratio. We note that our results may be somewhat specific to the CCS, and that the magnitude of change (and trends in specific variables) projected by HadGEM2-ES can differ considerably to that projected by other ESMs and within other systems (Pozo Buil et al. 2021). However, the directionality of projected change in offshore waters, which are the focus of this study, are consistent across three ESMs examined in Pozo Buil et al. (2021).

Generating the species distribution and abundance

We based the simulated species on a pelagic predator which responds to sea-surface temperature (SST), prey fields, and mixed layer depth (MLD) in the CCS, and is present during spring. We chose to model our species to resemble a large pelagic predator (e.g. characteristics similar to albacore (*Thunnus alalunga,* Scombridae) or swordfish *(Xiphias gladius,* Xiphiidae) because these species have high capacity to follow changing environmental conditions, potentially leading to greater future issues with cross-boundary management, viability of home-ports, bycatch interactions, and other consequences of climate-induced range shifts (Smith et al. 2021b). In addition, large pelagic predators are commercially-important species for US West Coast fishermen (Frawley et al. 2021) but are not routinely sampled as part of fisheries-independent surveys.

Spatial biomass of our virtual pelagic predator was simulated through a two-step process (Brodie et al., 2020). First, we simulated habitat suitability based on environmental and biological data and defined species preferences (Fig S7; see supplementary methods and Table S1 for more detailed information on species preferences). The environmental and biological variables used to force the species habitat suitability were SST (˚C), MLD (m) and the distribution of a simulated prey species, which was forced by SST and zooplankton biomass integrated over the upper 200 m of the water column (mmol N m^{-2}). We chose to focus on the spring season, when temperatures typically warm rapidly in the northern CCS. Each variable was therefore averaged over the spring months (March - May) to capture typical spring conditions in the study system.

Second, habitat suitability for the simulated species was converted into presence-absence using the *probability* method in *virtualspecies.* This approach does not use a defined threshold or cutoff for presence-absence. Instead, it uses a logistic function to convert the environmental suitability of each cell into a probability of occurrence. The probability of occurrence is then used to sample presence-absence in each cell using a random draw that is weighted by the probability of occurrence (Meynard et al. 2013, Leroy et al. 2016). Biomass (kg) was then calculated as a function of the habitat suitability at locations where it was classified as present, and determined to be 0 where the species was classified as absent, for each year of the simulation. Specifically, biomass was estimated from a log-normal distribution estimated from albacore (the model species for our simulated large pelagic predator) biomass in the CCS, and when the species was present, biomass at each grid cell was multiplied by habitat suitability of that same grid cell to provide habitat-informed biomass (see Table S1). Albacore biomass in the CCS was considered as the average biomass vulnerable to the U.S. surface fleet from 1999-2015 (Tommasi and Teo 2020).

Sampling Process: simulating fishery-dependent data collection

We sampled the simulated species distribution according to 14 different sampling scenarios which fall under five general types of sampling types: random sampling (1 scenario), preferential sampling (1 scenario), constrained by distance to port (8 scenarios), constrained by bycatch avoidance (1 scenario), and constrained by a closed area (3 scenarios). To determine the locations of fishing activity for each of the scenarios, except *Random,* we built a 'fishing suitability' raster using a similar process as was used to build the habitat suitability rasters for our simulated species as described previously. The fishing suitability raster was used to determine the probability of each cell being sampled using the 'weights' feature within the *sampleoccurrences* function in the *virtualspecies* package. Below is an overview of the different sampling scenarios, and the full details of the generation of these fishing suitability rasters are given in Supplemental materials, Material S1.

1) Random sampling: This represents our control, unbiased scenario, and is closest to fishery-independent sampling. In this scenario, each cell within our study area (ROMS

domain) has an equal probability of being sampled regardless of the underlying abundance of the virtual species.

2) Preferential sampling: The probability of a cell being fished is a function of the habitat suitability for the target species in the previous year (y-1), where the greater the habitat suitability the higher the probability of fishing occurring.
3) Constrained by distance to port: Suitable fishing areas are determined by distance to home ports and habitat suitability for target species. We built fishing suitability rasters for 8 different distance from port scenarios: two where fishing was limited to just around northern CCS ports (Ports Northern), two limited to around ports in the middle of the ROMS domain (Ports Middle), two limited to around southern ports (Ports Southern), and two which were not limited (e.g., fishing enabled around all ports; Ports All). One of the scenarios for each pair simulated an offshore fishery where fishing suitability was high up until about 300 miles from a port (Offshore), and one scenario simulated a nearshore fishery where fishing suitability declines after about 50 miles from a port (Nearshore).
4) Constrained by bycatch avoidance: Suitable fishing areas are determined by habitat suitability of the target species, while avoiding areas of high bycatch risk (e.g. high habitat suitability for simulated bycatch species).
5) Constrained by closed area: Suitable fishing areas are determined by habitat suitability of the target species, while taking into account that no fishing activity can occur within a static closed area. We built fishing suitability rasters for three closed area scenarios in which the size of the closed area varied (referred to as Closed Area Small, Closed Area Medium, and Closed Area Large).

These five general types represent simplified behavior observed in actual fisheries, including some on the U.S. West Coast. Preferential sampling represents the most ubiquitous fisher behavior, whereby fishers follow their target species to maximize profitability (van Putten et al 2012). Distance to port sampling is observed in the Pacific sardine fishery (Rose et al 2015, Smith et al 2021a), and closed area and bycatch avoidance sampling is observed and expected in the drift gillnet swordfish fishery (Urbisci et al 2016, Hazen et al 2018). We note that fishery-dependent data arises from additional processes beyond those included in the simulation model

here (e.g., vertical distribution, vessel attributes, targeting and reporting rates in multispecies logbooks, area vs. effort expansion, etc.), and that there is a large literature on dealing with those additional complexities that we do not address in the SDMs fit in this study (Stephens and MacCall 2004, Maunder and Punt 2004, Maunder et al. 2021).

Estimation models: fitting species distribution models

We fit the simulated data using two types of SDMs commonly used in ecological modeling: a correlative statistical model (generalized additive model, GAM; *mgcv* R package, Wood 2017) and a machine learning model (boosted regression tree, BRT; *gbm* R package, Elith et al. 2008). All SDMs were constructed as delta models, in which separate models are used to model the encounter probability (presence-absence) and the expected abundance conditional on encounter. All SDMs were trained on data from years 1985-2010, which we refer to as the 'historical' period, and then the fitted models were used to predict species biomass using projected environmental data for years 2011-2100. The SDMs were fit including three environmental covariates (SST, MLD, surface chlorophyll-a) (Table S2). We use surface chlorophyll-a instead of the distribution of prey or zooplankton to avoid a perfectly specified model and mimic real-world conditions where some environmental correlates are imperfectly known. The distribution of the virtual species in the OM is directly influenced by SST, MLD, and the distribution of its prey species which is influenced by zooplankton and SST. The SDMs include SST and MLD, but include surface chlorophyll-a as an indirect and imperfect proxy for prey or zooplankton. Because satellite-derived chlorophyll-a data are typically available (and prey and zooplankton data are not), this also approximates how similar models might be applied in a real-world scenario.

We evaluated the impact of alternative parameter configurations, such as including space and time covariates, on the relative influence of the different sampling scenarios on SDM performance (see Table S2 for the alternative configurations explored), but including these covariates added little to explained information (Table S2), and did not improve the spatial patterning in residuals (Fig. S1), or alter the relative impact of the different sampling scenarios on model performance (Fig. S2). This was likely due to the fact that the structure of our operating model could be well explained by dynamic ocean variables, and did not contain much

spatially-structured residual information, such as known spawning grounds. Therefore, we only present and discuss the results of the BRT and GAM environmental covariate models throughout the rest of this paper.

Assessment of Climatic Bias in the Sampling Scenarios

In order to assess the potential biases in estimates of environmental conditions created by fishery-dependent sampling, we assess both the climatic bias and climatic novelty. The climatic bias compares the sampled environmental conditions to environmental conditions throughout the entire ROMS domain during the historical sampling period (1985-2010). Climatic novelty is a measure of how similar the environmental conditions captured in each of the sampling scenarios are to the projected future environmental conditions present across the entire domain (i.e., a measure of extrapolation).

We used two metrics to obtain climatic bias and novelty, Cohen's *d* (cd) and Hellinger Distance (HD). Cohen's *d* is a measure of the distance between the means of two groups, while the HD is a measure of the difference between two probability distributions (see Legendre & Legendre 2012; Supplemental Methods for formulas). The HD measures how much information is contained in one distribution relative to another with values in the range [0,1]. Values of HD = 1 indicates that the two distributions have no common information (e.g., no data overlap), whereas values of HD = 0 indicates that the two distributions have the same information (e.g., complete data overlap). Johnson and Watson (2021) propose HD values > 0.5 as a threshold of novelty, where the distributions become more dissimilar than they are similar. We used both of these two metrics because while Cohen's *d* can quantify the direction and magnitude of the difference between means, it does not capture differences in the shape of the distributions. In contrast, though HD does not capture the direction of the difference, it can measure differences in the mean and shape of distributions. Therefore, the two metrics combine to provide an overall picture of the climatic bias and novelty.

Model Performance: predicting abundance, center of gravity, and spatial distribution

Model estimates for species abundance and center of gravity were compared to the simulated data, which represents the known truth, and fit and performance were evaluated using

several metrics, including root mean squared error (RMSE) and Spearman correlation coefficient for continuous metrics, and the area under the receiver operating characteristic curve (AUC) for the presence/absence portions of the SDMs. AUC is a common metric to assess SDM accuracy, with values > 0.75 suggesting the model provides good discrimination between locations where the species is present and where it is absent (Elith et al. 2006). SDM outputs were also compared by visually examining the predicted spatial distributions, and the model response curves for each environmental covariate (Supplementary material). For comparing performance through time, we broke the future period into three timeframes, early-century (2011-2039), mid-century (2040-2069) and late-century (2070-2100).

RESULTS

Environmental Variability, Sampling Scenario Climatic Bias, and Novelty

The environmental variables used in the operating and estimation models exhibited both spatial and temporal variability. Surface chlorophyll, zooplankton, and MLD showed a nearshore-offshore gradient, with surface chlorophyll and zooplankton concentrations being greater nearshore, while MLD was greater offshore (Fig. 3). Temperature exhibited a north-south gradient, with higher temperatures in the southern portion of the domain during the historical period, but increasing throughout the domain during the future period (Fig. 3). In general, MLD, zooplankton, and surface chlorophyll all decreased during the projection period (Fig. 3). The simulated species biomass built using these environmental variables (i.e., in the operating model) also showed strong spatial patterning, and was higher in southern and offshore waters. During the projection period, biomass of the simulated species increased in the northern part of the domain and decreased in the southern portion.

The geographic spatial pattern of the different sampling scenarios varied within the ROMS domain (Table 1, Fig. 4), leading to differences in the environmental conditions captured in their samples. The random sampling scenario, not surprisingly, covered the largest geographic area, covering almost 90% of the ROMS domain (Table 1, Fig. 4,), resulting in a wide range of environmental conditions being sampled, and the lowest climatic biases across all environmental parameters (Table 1, Fig. 5). The most biased designs were the distance from port sampling scenarios, particularly the Northern Ports Only and Southern Ports Only sampling regimes,

400 followed by the nearshore pair of the Middle Ports and All Ports Only scenarios (Table 1, Fig. 5).
401 These sampling scenarios were the most limited in their geographical coverage, being restricted
402 latitudinally and/or longitudinally (i.e., in the nearshore-offshore direction). Additionally, the
403 Northern Ports Only sampling scenarios were cold-biased (cd = 0.47 and cd = 0.73) with greater
404 sampling effort at the low temperatures and poor sampling at the high temperatures, whereas the
405 Southern Ports Only sampling scenarios were warm-biased (cd = -0.71 and cd = -0.97) (Table 1,
406 Fig. 5, Fig S2) with greater sampling at the high temperature extremes.
407
408 In general the environmental conditions became increasingly novel over time relative to
409 the environmental conditions represented in each sampling scenario during the historical period
410 (Table 2, Fig. 5). For all sampling scenarios except Ports Southern Nearshore and Offshore, the
411 climate novelty (HD and Cohen's *d*) increased through time for chlorophyll and temperature,
412 with the largest climate novelty occurring in the late-century period (Fig. 5, Fig S3-5; Table 2),
413 while climate novelty (HD and Cohen's *d*) for MLD remained low and relatively unchanged for
414 all future time periods (Table 2). In the early-century (2011-2039) environmental conditions
415 were novel for at least one environmental variable used in the estimation model relative to the
416 conditions captured by three of the sampling scenarios, Ports Northern Nearshore, Ports Northern
417 Offshore, and Port Southern Nearshore. In the mid-century (2040-2069) the conditions became
418 less novel relative to the Port Southern Nearshore sampling data, but we saw the emergence of
419 novel conditions relative to the Middle Ports Nearshore sampling scenario for two environmental
420 variables (temperature and chlorophyll; Table 2) and an increase in novelty relative to the Ports
421 Northern Nearshore and Offshore scenarios. By the late-century period (2070-2100), temperature
422 conditions were approximately novel (HD ~ 0.5) and warmer (Fig. 5, bottom panel, Table 2)
423 than captured by all of the sampling scenarios during the historical period. Additionally,
424 conditions were novel for two environmental parameters (temperature and chlorophyll) for four
425 sampling scenarios, Ports Northern Nearshore and Offshore, Port Middle Nearshore, and Ports
426 All Nearshore during the late-century period (Table 2). The Ports Southern Nearshore and
427 Offshore sampling scenarios are unique in that the HD was > 0.5 for temperature during the
428 historical sampling period (Fig. 4, top panels), but then declines into the early- and mid-century,
429 before increasing slightly again in the late-century period. While the southern sampling scenarios

were warm biased relative to historical temperatures throughout the entire prediction domain, those warm biased temperatures become more representative of the full domain in the future.

SDM Model Fit and Predictive Skill

SDMs generally fit well to the presence-absence training data generated from the simulated fishery-independent and fishery-dependent sampling scenarios with all AUCs > 0.78 for the BRTs (Araujo et al. 2005; Table 1). However, there was a noticeable difference in the predictive performance for models fit to data from the Southern Nearshore and Offshore sampling scenarios, particularly for the GAMs. Most sampling scenarios tracked the true abundance well during the historical period, except for the two Southern Ports Only scenarios which overestimated the true abundance (Fig. 6). The Ports Southern Nearshore model had the lowest AUC values (0.54 and 0.78 for the GAM and BRT respectively; Table 1). One would not normally project a model which had an AUC of 0.54 as that indicates poor fit (Elith et al. 2006; Araujo et al. 2005; Swets 1988), however, we retained the model for the purposes of this simulation.

The ability of the SDMs to replicate the known environmental affinities of the simulated species was best for models fit with the less climatically-biased sampling designs (Figs. S7-S14). However, only the Random and Ports Southern Nearshore sampling scenarios were able to predict the dome response curve for temperature, while other scenarios overpredicted the positive impact of high temperatures on the virtual species abundance (Fig S7-S8). The fitted response curves generated through all other scenarios showed increasing positive partial effects on biomass at high temperatures, instead of the decline observed in the true species response curves above 17 degrees C. This result was most pronounced for the Ports Northern Offshore, Northern Nearshore, and Middle Nearshore sampling scenarios, which is likely due to the fact that these scenarios sampled were cold-biased (positive cohen's d; Table 1), sampling only low to mid temperature waters, and did not capture the higher temperature ranges. Models fit to data from the Ports Southern Nearshore scenario, however, were better able to capture the species temperature preferences at higher temperatures, but not at lower temperatures (Fig S6-S7).

SDM Projection Performance

In our study, model performance (RMSE) tended to decline with increasing HD (Figure S15), and in general, SDM performance (as determined by RMSE, correlation, model uncertainty, and spatial error) was the worst during the period when climatic bias and novelty was greatest. For most scenarios this occurred during the late-century period, but for the two Southern Ports Only scenarios it was during the historical training period.

Many of the models fit to data collected from a fishery-dependent sampling scenario (Preferential, Bycatch, Closed Area Small, Closed Area Medium, Closed Area Large, Ports All Offshore, Ports Middle Offshore) performed comparably to the Random sampling scenario, tracking the true biomass well during the early- and mid-century projection periods (Table 3, Fig 6a,b). However, these sampling scenarios exhibited a more pronounced decline in performance (increasing RMSE (Table 3, Fig S16), decreasing correlation (Fig S17), and increasing uncertainty (Fig S18)) during the late-century period compared with the random sampling scenario (Table 3). Models built with more climatically biased training data performed less well. The worst performing models were those fit to data collected from the Ports Northern Nearshore, Ports Northern Offshore, Ports Middle Nearshore, Ports Southern Nearshore, and Ports Southern Offshore sampling scenarios (Table 3, Fig. 6a,b). An interesting observation, however, is that while performance declined throughout the projection period for Ports Northern Nearshore, Ports Northern Offshore, and Ports Middle Nearshore, it improved somewhat for the Ports Southern Offshore and Ports Southern Nearshore scenarios, probably because environmental conditions were actually becoming less novel (compared to those sampled) for the southern sampling scenarios.

Models that were best able to track biomass during the early and mid-century periods were also best able to track the true center of gravity during the early-century and beginning of the middle-century periods (Preferential, Bycatch, Closed Area Small, Closed Area Medium, Closed Area Large, Ports All Offshore, Ports Middle Offshore; Fig. 7a,b). These models predicted center of gravities within 1 degree latitude on average of the true center of gravity through the early and mid-century, before diverging from the true center of gravity trend and

beginning to underestimate the northward shift by more than 1 degree during the late-century periods (Fig. 7b). The most highly climatically biased scenarios (Ports Middle Nearshore, Port Northern Nearshore, and Port Northern Offshore) on the other hand began underestimating the true center of gravity by more than 1 degree starting in the mid-century and by the late-century they underestimated the true center of gravity by as much as 2.4-3.2 degrees. The Southern Nearshore and Offshore scenarios were unique in that they overestimated the center of gravity by almost 2.6-2.7 degrees during the historic period and then underestimated the center of gravity throughout the future periods (Fig 6b).

Spatially explicit predictions of biomass were also comparatively similar across sampling procedures and resembled the true abundance distribution during the historical and early and mid-century future periods (Fig. 8; Figs S19-S22). In the late-century period, all sampling scenarios overpredicted the true biomass in the southern, warmer part of the CCS. The exception to this was models fit to data collected under the Ports Northern Nearshore, Ports Northern Offshore, Ports Middle Nearshore and Ports All Nearshore sampling scenarios, which overpredict the biomass of the species in the southern part of the ROMS domain throughout the entire time series, with the greatest overpredictions in the late-century period. Additionally, models fit with data collected under the Ports Southern Nearshore and Offshore sampling scenarios overpredict the biomass in the northern part of the domain throughout the time period (Fig. 8, Figs S19-S22), as well as overpredicting the biomass in the southern part in the middle- and late-century. Again, this likely occurred because models fit with Southern Ports Only data do not accurately represent the species temperature response curve at lower temperatures; similarly, models fit using the other sampling scenarios do not accurately represent the species temperature response curve at intermediate and higher temperatures, and this is particularly true for the two Northern Only and the Middle Nearshore Ports scenarios.

DISCUSSION

As climate change leads to increasingly novel ocean conditions (Gruber et al 2021; Smith et al. 2022), it is important to understand how fish and other marine organisms will respond to those changes. Realistic projections of potential future species distributions are important to categorize species responses, and to be able to prepare for and sustainably manage for

distribution shifts. However, there is limited understanding of how well models perform when projecting decades into the future, particularly when training data come from varied sources, such as with fishery-dependent data. In this study we showed that use of non-randomly sampled data can have relatively minor impact on SDM performance for near- to medium-term projections as long as it samples well the underlying environmental conditions present. We further established that, regardless of sampling design, SDM performance tends to degrade for long-term projections (RMSE = 5.5 - 8.6 vs. RMSE = 5.3 - 12.6, during early- and late-century respectively), due to the higher climatic novelty of the future environmental conditions relative to the sampling data.

Differences Among Sampling Scenarios

A major concern with fishery-dependent data used to estimate species distributions is the potential biases due to the unequal sampling, as fishers tend to preferentially target locations with high density of specific fishes and respond to external economic and management factors rather than randomly sampling. However, our results show that data generated from fishery-dependent sampling can still result in SDMs with performance comparable to SDMs generated from random samples several decades into the future, given specific forms of preferential sampling which result in low climate bias and novelty (e.g., HD < 0.5). Preferential, Closed Areas, Bycatch, and Ports Middle Offshore, Ports All Offshore all had low climate bias in the training data, and models fit to these data performed similarly to each other, and to the Random sampling scenario before degrading around mid- to late-century (e.g., RMSE 5.55 - 6.99 vs 5.47 - 5.5 respectively). On the other hand, the Southern Ports Only and Northern Ports Only scenarios had the highest climate bias or novelty and performed poorly throughout the projection period. By evaluating our range of scenarios, generalizations can be made about the causes of poor SDM performance and magnitude resulting from biased sampling. These generalizations relate to how well fishery-dependent data leads to correctly specified species-climate response curves, and how well these data represent the environmental conditions that exist in the data set used for prediction.

Our findings were consistent with numerous studies which show that restricting the range, and particularly the extremes, of environmental data present in a sample can affect the calculation of species-climate response curves, and can lead to erroneous projections (Thuiller et al. 2004, Hortal et al. 2008, Tessarolo et al. 2014, Stoa et al. 2018, Nazzaro et al. 2021). This is likely to occur in systems with strong geographic or temporal gradients in environmental variables when only a portion of the domain or a portion of the habitat or only certain seasons or years are sampled. For example, this was particularly evident for the Northern Ports Only and Southern Ports Only scenarios, where the environmental range covered in the samples was restricted to either cold (northern ports) or warm (southern ports) waters. This led to inaccurate prediction of the species responses to warm temperatures for the northern ports scenario, and to cold temperatures for the southern port scenario. If a response to a particular environmental covariate is non-linear (e.g. our domed preference for SST, Table S1), high sampling coverage across a range of covariate values may be required to fit that response correctly. Often there will be reduced data coverage and increased model uncertainty at the limits of this response. This uncertainty will be exacerbated if extrapolation of this response is required during prediction or projection, which can be seen in our study in Figure S18. Therefore, one should be careful or critical when an estimated relationship to an environmental variable is approximately linear across the training data, particularly if it is a positive linear relationship.

Training data quality is also acknowledged to be a key issue determining the transferability of SDMs to novel locations or environments (Elith & Leathwick 2009; Yates et al. 2018). We measure this as both climatic bias (how well the historical climate was sampled in our domain of interest) and climatic novelty (how well the sampled historical climate represents future conditions used for projection). We also estimated the spatial area covered by each sampling scenario (Figure 4), and this tended to be a good indicator of the subsequent climatic bias, with scenarios that sampled a higher proportion of the ROMS domain, tending to have lower climatic bias of the sample; however, this was not always the case (Table 1). This is consistent with previous studies which conclude that the underlying environmental conditions sampled is more important than the spatial structure of samples in terms of effecting SDM performance (Tessarolo et al. 2014), and supports the use of a climatic bias measure, such as the

HD, as a metric of data quality and potential indicator of SDM performance rather than the spatial coverage of a sample set.

Higher climatic bias in the sample data led to either poorly fit models (e.g., Southern Port Nearshore, AUC = 0.53, RMSE average = 9.34) and/or poor performance, and more quickly degrading performance, when projecting into future, novel conditions. Models fit to data from sampling scenarios with high climatic bias during the training period (Northern and Southern Ports only, Middle Nearshore, and All Nearshore) resulted in RMSEs during the early and mid-century period that were 14-75% greater relative to random sampling, whereas the less climatically biased scenarios resulted in RMSE that were only 1-18% greater compared to the random sampling scenario. By the late century period all SDMs except for those fit to the Random sampling scenario showed declining performance; however this decline in performance was greater for the more climatically biased sampling with RMSE increasing to 33-128% greater than the random sample compared with only 11-56% greater for less biased scenarios. This suggests that SDMs will likely show degrading performance over time given high climatic novelty in future periods, although random sampling can help mitigate this (Fig. 6; Table 3). We note that the amount of extrapolation into the future, and thus the impact on model predictive skill, varies among climate models (see Brodie et al. 2022) and scenarios. In our simulation we used the HadGEM2-ES ESM, which exhibits some of the fastest warming and productivity declines for the CCS (Pozo Buil et al., 2021) and thus higher novelty (Smith et al, in press). Thus, while in our study SDM projection performance began to degrade mid-century for many scenarios, other studies may see performance degrade earlier or later depending on which ESM is used (Brodie et al., 2022). Our results suggest that this degradation in performance may occur when the conditions for at least one climatic variable used in the model become more dissimilar than similar (i.e. HD ~ 0.5) to the conditions represented in the training data.

Our results are based on a simplified simulation framework designed to test the predictive performance of SDMs fit to simulated fishery-dependent data, and as such there are several important assumptions and caveats to note. First, the scenarios simulated in our study are a simplified version of fishery-dependent data collection. There are several factors that we have not captured in our simulation which can impact both where and how much fishermen catch

(e.g., density dependence, interspecific interactions, catchability, fisher behavior, market dynamics), and therefore the relative bias and performance of models fit to that data. Future studies could work to incorporate these dynamics into simulations. Additionally, we simulated a mobile pelagic species, which has the advantage of not having to consider benthic habitat requirements (the animal can just move to follow favorable conditions). Simulating benthic or demersal species realistically might be more difficult. Additionally, how a species is distributed in space and time can be determined by more than just environmental conditions. Other important drivers could include, life history and the complexity of the life cycle, the presence of specific habitat requirements, trophic interactions, and competition. For example, a diadromous species exhibiting natal homing may have clear thermal and other environmental preferences but have less ability to shift its distribution than a species which completes its entire lifecycle in the epipelagic zone. Exploring the impact of these additional drivers of species distributions on SDM performance given different sampling scenarios is beyond the scope of this study, but may be a fruitful endeavor for future simulations. Lastly, while our simulation focuses on the CCS, the general conclusions with regard to the relationship between the climatic bias of the training data and climatic novelty of the future conditions and performance of SDMs can be of use to other systems. However, we would expect that the specific sampling patterns that may lead to climatically biased data will depend on the spatial gradient of the environmental conditions and factors influencing species distributions and fishing patterns within a specific system.

Applications and Recommendations

Although fishery-dependent data are inherently biased, they can still be useful for SDMs and projection, especially if we can account for this bias through careful model specification or by restricting predictions to the geographical or environmental space covered by the model training data (e.g., Crear et al. 2021). For example, warming is one of the key climate drivers in long term projections. If our fishery-dependent observations cover a broad range of a species' thermal tolerance, and if the behavior of the SDM near the upper thermal limit corresponds well with known physiological limits, then projections of habitat change due to warming are likely to be more accurate. This also applies to other important environmental drivers, such as dissolved oxygen and pH, and is in line with Elith et al. (2011) and Stoa et al. (2018) which posit that good

SDM performance relies on the distribution of the sampling effort being proportional to the actual frequency distribution of environmental conditions along all environmental variables of importance to the species; which can be indicated through the use of the HD and cd as done in this study. On the other hand, an SDM is less likely to provide realistic projections if the observations sample a relatively small portion of the species geographic or environmental range, if detectability on fishing gear is imperfect or inconsistent, or if SDM covariates do not represent key processes well (such as obligate prey following or other trophic interactions that are not directly linked to environmental variables).

We have shown that climatic bias and novelty are useful measures of impact of available observations on the performance of SDM projections. These or similar metrics (Mesgaran et al. 2014, Meyer and Pebesma et al. 2021, Smith et al. 2022) are critical components of projection studies because they allow estimation of how no-analog environmental conditions relate to predictive skill. However, consideration of how different modeling methods behave when extrapolated is also essential, as some are better suited to extrapolation. The two methods used in this study (BRTs and GAMs) predict to novel conditions differently. GAMs (depending on how they are parameterized) can continue fitted trends into new environments, whereas BRTs assume a constant relationship outside of the training data range (Zurrell et al. 2012). Our results show that GAM and BRT projections often diverged strongly towards the end of the 21st century for more biased sampling scenarios, as environmental conditions became more novel. Although this is particular to our study, projections from BRTs were generally closer to the simulated truth, probably because of their more conservative behavior under extrapolation. Other studies (e.g. Zurrell et al. 2012; Moore et al. 2016; Derville et al. 2017) indicate that BRTs do not always outperform GAMs, and that the best SDM for a particular purpose tends to be highly species- and ecosystem-specific. Overall, the use of an ensemble of different SDMs is likely useful for capturing some of the uncertainty contributed by model extrapolation behavior when predicting in novel environments. Predictions from different types or parameterizations of SDMs can be ensembled, and weighted based on some measure of model fit or uncertainty (e.g., Yao et al. 2018)

Accounting for bias in fishery-dependent data through model specification has a rich history, driven by models aimed at catch-per-unit-effort standardization and calculating

673 abundance indices (Thorson et al. 2020, Maunder and Punt 2004). Spatial and temporal biases in
674 these data (such as a spatial shift in fishing effort) are often accounted for by including spatial
675 and temporal covariates (Ducharme-Barth et al. 2022), which are used to explain unknown
676 biological processes, or to act as latent variables to explain residual dependencies. These studies
677 focus on standardizing observed data to explain historic patterns of spatial distributions and
678 abundance. However, these spatial-temporal standardization tools may be unsuitable for long
679 term projection of species distributions, given that static spatial surfaces and covariates
680 incorporating year effects used to explain the past may not extrapolate well to future conditions.
681 Indeed, some covariates can act as surrogates for variables or processes that may diverge over
682 time and result in poor projections of species distributions. And yet, the benefits of spatial-
683 temporal modeling not only include the potential to reduce bias in fishery-dependent
684 observations, but also the 'borrowing' of nearby information to improve the accuracy of spatial-
685 temporal extrapolation (Thorson 2019 [VAST]; Brodie et al. 2020). We note that when we
686 evaluated the impact of including space and time covariates on the relative influence of the
687 different sampling scenarios on SDM performance, including these covariates added little to
688 explained information (Table S3), and did not improve the spatial residual pattern (Fig. S1) or
689 alter the relative impact of the different sampling scenarios on model performance (Fig S2).
690 However, there is potential for other parameterizations of the space and time covariates to have
691 different results, and considering the potential benefits and successes in reducing bias seen in
692 other studies, further exploring the use of spatio-temporal modeling for SDMs using fishery-
693 dependent data is still warranted. Another approach that has shown promise to reduce bias from
694 preferential sampling data is to use a modeling framework where the state variable of interest
695 (e.g., population biomass or abundance) and the sites chosen for sampling are jointly modeled
696 using a dependence covariance matrix (Conn and Thorson 2017). Future work could also
697 consider this analytical approach to explicitly account for biases from fishery-dependent
698 sampling.
699
700 The challenge remains, then, to decide how much extrapolation in time (years or seasons)
701 or space is acceptable, and these variables can be included in measures of novelty (Smith et al.
702 2022) to aid this decision. However, in terms of projecting into novel conditions, geographic and
703 temporal separation between the reference and target system appears less important compared

with environmental dissimilarity (Yates et al. 2018). In this paper we show how Hellinger Distance can be used as a measure of this environmental dissimilarity, with values around the 0.5 threshold proposed by Johnson and Watson (2022) serving as an indication of when projections (transferability) may become problematic. Again, we note that the amount of extrapolation into the future that might be appropriate may vary among climate models, and exploring the dissimilarity (or similarity) in future climate projections could be informative to future management scenario planning.

When projecting SDMs built from fishery-dependent data, we recommend to: 1) collect training data from the broadest range of environmental conditions relevant for a species (Pennino et al. 2016), which may require combining fishery-independent and dependent data sets (e.g. Rufener et al 2021, Alglave et al. 2022); 2) use one or more diagnostics to identify biased data, severe extrapolation, and potentially inaccurate predictions (e.g., our Hellinger D threshold); 3) evaluate the plausibility of the partial species-climate responses, especially at the limits of the fitted data and when extrapolated to novel data; 4) explore spatio-temporal modeling, and other analytical approaches, to reduce bias in training data, but evaluate the benefits against the reduced flexibility of spatial-temporal variables for long-term projection; 5) measure and communicate uncertainty of projections, but recognize that if data are biased and a model is poorly specified then uncertainty may be underestimated.

CONCLUSION

We show that SDMs built using data collected from a simulated fishery can produce projections of species distributions similar to SDMs fit with data collected from a random sampling scheme, as long as the sampling adequately captures the underlying environmental conditions present in the prediction domain. Being able to diagnose and understand when fishery-dependent data is of high enough quality (e.g., low climate bias and novelty, in addition to accurate location and catch reporting) to produce accurate predictions can help open the door for scientists and managers to use more of the observational data available to them, and to more fully understand the uncertainty associated with using this data for predictions and projections of species distributions.

The use of fishery-dependent data, either on its own or in conjunction with fishery-independent data, has several benefits. For example, fishery dependent data are often collected at higher spatial and temporal resolutions than fishery independent survey data. Unbiased fishery dependent data (e.g., with low climate bias and novelty), or fishery-dependent data bias corrected through the use of spatio-temporal modeling as discussed above or other bias correction approaches, may thus be our best way of linking fish distributions to seasonal and spatial processes such as physical drivers of recruitment (e.g., preconditioning of mature females; Tolimieri et al. 2018, Haltuch et al. 2020) or seasonal/long term changes in habitat characteristics like temperature, dissolved oxygen, stratification, seascape characteristics (Pennino et al. 2016). Additionally, having distribution data from many seasons will help to parameterize seasonal species distribution expectations in end-to-end models that support ecosystem-scale management strategy evaluations, e.g., focused on robustness of management structure to species distribution shifts driven by climate events and climate change (Kaplan et al. 2021). Synthesizing outcomes across fishery-dependent and independent data can help support the Ecosystem-Approach to Fisheries Management (EAFM) or Ecosystem-Based Fisheries Management (EBFM), through incorporating fishers' knowledge (e.g., local ecological knowledge) along with any additional data they may be able to collect in the future as ships-of-opportunity for monitoring environmental conditions. Finally, as costs and financial resources for fishery-independent surveys are increasingly limited in many areas, fishery-dependent data may be able to supplement information from surveys that are reduced or eliminated for budgetary reasons (though not without potential cost to the usefulness of the data).

DATA AVAILABILITY

The ROMS-NEMUCSC projection data were developed by Pozo Buil *et al.* 2021, and are available upon request from Mercedes Pozo Buil, or from NOAA's ERDDAP data servers at the following URL: https://oceanview.pfeg.noaa.gov/erddap/search/index.html?&searchFor=CCS+ROMS. The R code to run the simulation can be found on GitHub (https://github.com/Melissa-Karp/Fishery-dependent-SDM-projections).

ACKNOWLEDGEMENTS

We would like to thank Chris Harvey, Caren Barcelo, Jim Thorson, John Best, Carey McGilliard, Dan Crear, and Kisei Tanaka for their comments and feedback on earlier versions of this paper. This study arose from a workshop in support of the Western Regional Action Plan of the NOAA Fisheries Climate Science Strategy, with assistance from the California Current IEA.

REFERENCES

Araujo, M. B., Pearson, R., Thuiller, W., & Erhard, M. (2005). Validation of species–climate impact models under climate change. *Global Change Biology,* 11, 1504–1513. https://doi.org/10.1111/j.1365-2486.2005.01000.x

Baker, D. J., Maclean, I. M. D., Goodall, M., & Gaston, K. J. (2022). Correlations between spatial sampling biases and environmental niches affect species distribution models. *Global Ecology and Biogeography*, 31, 1038–1050. doi:10.1111/geb.13491

Becker, E. A., Forney, K. A., Redfern, J. V., Barlow, J., Jacox, M. G., Roberts, J. J. & Palacios, D. M. (2019). Predicting cetacean abundance and distribution in a changing climate. *Diversity and Distributions*, 25(4), 626-643. https://doi.org/10.1111/ddi.12867

Brodie, S. J., Thorson, J. T., Carroll, G., Hazen, E. L., Bograd, S., Haltuch, M. A., Holsman, K. K., Kotwicki, S., Samhouri J. F., Willis-Norton, E., & Selden, R. L. (2020). Trade-offs in covariate selection for species distribution models: a methodological comparison. *Ecography*, *43*(1), 11-24. https://doi.org/10.1111/ecog.04707

Bucaram, S. J., White, J. W., Sanchirico, J. N., & Wilen, J. E. (2013). Behavior of the Galapagos fishing fleet and its consequences for the design of spatial management alternatives for the red spiny lobster fishery. *Ocean & Coastal Management*, 78, 88– 100. https://doi.org/10.1016/j.ocecoaman.2013.03.001

Cheung, W. W., Lam, V. W., Sarmiento, J. L., Kearney, K., Watson, R., & Pauly, D. (2009). Projecting global marine biodiversity impacts under climate change scenarios. *Fish and Fisheries,* 10, 235–251. https://doi.org/10.1111/j.1467-2979.2008.00315.x

Cheung, W. W., Brodeur, R. D., Okey, T. A., & Pauly, D. (2015). Projecting future changes in distributions of pelagic fish species of Northeast Pacific shelf seas. *Progress in Oceanography*, 130, 19-31. https://doi.org/10.1016/j.pocean.2014.09.003

Cohen, J. (1988) Statistical power analysis for the behavioral sciences. Lawrence Erlbaum Associates, Inc., Hillsdale, NJ

795 Conn, P. B., Thorson, J. T., & Johnson, D. S. (2017). Confronting preferential sampling when
796 analysing population distributions: diagnosis and model-based triage. *Methods in Ecology*
797 *and Evolution*, *8*(11), 1535-1546. https://doi.org/10.1111/2041-210X.12803

798 Crear, D. P., Curtis, T. H., Durkee, S. J., & Carlson, J. K. (2021). Highly migratory species
799 predictive spatial modeling (PRiSM): an analytical framework for assessing the
800 performance of spatial fisheries management. *Marine Biology*, 168.
801 https://doi.org/10.1007/s00227-021-03951-7

802 Daw, T. M. (2008). Spatial distribution of effort by artisanal fishers: Exploring economic
803 factors affecting the lobster fisheries of the Corn Islands, Nicaragua. *Fisheries Research*,
804 90, 7-25. doi:10.1016/j.fishres.2007.09.027

805 Dennis, D., Plaganyi, v., Van Putten, I., Hutton, T., & Pascoe, S. (2015). Cost benefit of
806 fishery-independent surveys: Are they worth the money? *Marine Policy*, 58, 108-115.
807 https://doi.org/10.1016/j.marpol.2015.04.016

808 Derville, S., Torres, L. G., Iovan, C., & Garrigue, C. (2018). Finding the right fit: Comparative
809 cetacean distribution models using multiple data sources and statistical approaches.
810 *Diversity and Distributions*, 24(11), 1657-1673. https://doi.org/10.1111/ddi.12782

811 Diggle, P., Menezes, R., & Su, T.-I. (2010). Geostatistical inference under preferential
812 sampling. *Journal of the Royal Statistical Society: Series C (Applied Statistics)*, 59, 191-
813 232. doi:10.1111/j.1467-9876.2009.860 00701.x.

814 Ducharme-Barth, N. D., Gruss, A., Vincent, M. T., Kiyofuji, H., Aoki, Y., Pilling, G.,
815 Hampton, J., & Thorson, J. T. (2022). Impacts of fisheries-dependent spatial sampling
816 patterns on catch-per-unit effort standardization: A simulation study and fishery
817 application. *Fisheries Research*, 246, https://doi.org/10.1016/j.fishres.2021.106169

818 Elith, J., Leathwick, J. R., & Hastie, T. (2008). A working guide to boosted regression trees. J.
819 *Anim. Ecol.* 77: 802–813. https://doi.org/10.1111/j.1365-2656.2008.01390.x

820 Elith, J. & Leathwick, J. R. (2009). Species distribution models: ecological explanation and
821 prediction across space and time. *Annual review of ecology, evolution, and systematics*, 40,
822 677-697. https://doi.org/10.1146/annurev.ecolsys.110308.120159

823 Fiechter, J., Curchitser, E. N., Edwards, C. A., Chai, F., Goebel, N. L., & Chavez, F. P. (2014).
824 Air-sea CO2 fluxes in the California Current: Impacts of model resolution and coastal
825 topography. *Global Biogeochemical Cycles*, 28(4), 371-385. doi:10.1002/2013gb004683

826 Fiechter, J., Edwards, C. A., and Moore, A. M. (2018). Wind, Circulation, and Topographic
827 Effects on Alongshore Phytoplankton Variability in the California Current. *Geophysical*
828 *Research Letters*, 45(7), 3238-3245. doi:10.1002/2017gl076839

829 Frawley, T. H., Muhling, B. A., Brodie, S., Fisher, M. C., Tommasi, D., Le Fol, G., Hazen, E.
830 L., Stohs, S. S., Finkbeiner, E. M., & Jacox, M. G. (2021). Changes to the structure and
831 function of an albacore fishery reveal shifting social-ecological realities for Pacific
832 Northwest fishermen. *Fish and Fisheries*, 22(2), 280-297. https://doi.org/10.1111/faf.12519

833 Guisan, A. & Thuiller, W. (2005). Predicting species distribution: offering more than simple
834 habitat models. *Ecology Letters,* 8(9): 993-1009. doi: 10.1111/j.1461-0248.2005.00792.x

835 Gruber, N., Boyd, P. W., Frölicher, T. L., Vogt, M. (2021). Biogeochemical extremes and
836 compound events in the ocean. *Nature* 600, 395–407. https://doi.org/10.1038/s41586-021-
837 03981-7

838 Hazen, E. L., Jorgensen, S. J., Rykaczewski, R., Bograd, S. J., Foley, D. G., Jonsen, I. D.
839 Shaffer, S. A., Dunne, J., Costa, D. P., Crowder, L. B., & Block, B. A. (2013). Predicted
840 Habitat Shifts of Pacific Top Predators in a Changing Climate. *Nature Climate Change*
841 3:234-238. doi: 10.1038/nclimate1686.

842 Hazen, E. L., Scales, K. L., Maxwell, S. M., Briscoe, D. K., Welch, H., Bograd, S. J., Bailey,
843 H., Benson, S. R., Eguchi, T., Dewar, H., Kohin, S., Costa, D. P., Crowder, L. B., &
844 Lewison, R. L. (2018). A dynamic ocean management tool to reduce bycatch and support
845 sustainable fisheries. *Ecology* 4(5). doi: 10.1126/sciadv.aar3001.

846 Hortal, J., Jimenez-Valverde, A., Gomez, J. F., Lobo, J. M., & Baselga, A. (2008). Historical
847 bias in biodiversity inventories affects the observed environmental niche of the species.
848 *Oikos* 117:847–858. https://doi.org/10.1111/j.0030-1299.2008.16434.x

849 Howell, E. A., Kobayashi, D. R., Parker, D. M., Balazs, G. H., & Polvina, J. J. (2008).
850 TurtleWatch: a tool to aid in the bycatch reduction of loggerhead turtles *Caretta caretta* in
851 the Hawaii-based pelagic longline fishery. doi:10.3354/esr00096

852 Ishimura, G., Herrick, S., & Sumaila, U. R. (2013). Stability of cooperative management of the
853 Pacific sardine fishery under climate variability. *Marine Policy*, 39, 333–340.
854 https://doi.org/10.1016/j.marpol.2012.12.008

855 Johnson, S. M. & Watson J. R. (2021). Novel environmental conditions due to climate change
856 in the world's largest marine protected areas. *One Earth*, 4(11):1625-1634.
857 https://doi.org/10.1016/j.oneear.2021.10.016

858 Kadmon, R., Farber, O., & Danin, A. (2004). Effect of roadside bias on the accuracy of
859 predictive maps produced by bioclimatic models. *Ecological Applications*, 14: 401– 413.
860 https://doi.org/10.1890/02-5364

861 Kaplan, I. C., Gaichas, S. K., Stawitz, C. C., Lynch P. D., Marshall, K. N., Deroba, J. J., Masi,
862 M., Brodziak, J. K. T., Aydin, K. Y., Holsman, K., Townsend, H., Tommasi, D., Smith, J.
863 A., Koenigstein, S., Weijerman, M., & Link, J. 2021. Management Strategy Evaluation:
864 Allowing the Light on the Hill to Illuminate More than One Species. *Frontiers in Marine*
865 *Science*, 8:624355. doi: 10.3389/fmars.2021.624355

866 Kishi, M.J., Kashiwai, M., Ware, D.M., …. & Zvalinsky, V. I. (2007) NEMURO—a lower
867 trophic level model for the North Pacific marine ecosystem. *Ecological Modelling*, 202(1),
868 12-25. doi:10.1016/j.ecolmodel.2006.08.021

869 Legendre, P. & Legendre, L. (2012) Numerical Ecology, 3rd edn. Elsevier Science BV,
870 Amsterdam, NL.
871
872 Leroy, B., Meynard, C. N., Bellard, C., & Courchamp, F. (2016). virtualspecies, an r package to
873 generate virtual species distributions. *Ecography*, 39:599-607,
874 https://doi.org/10.1111/ecog.01388

875 Lynch, P. D., Shertzer, K. W., Cortes, E., & Latour, R. J. (2018). Abundance trends of highly
876 migratory species in the Atlantic Ocean: accounting for water temperature profiles. *ICES*
877 *Journal of Marine Science*, 75(4), 1427-1438. https://doi.org/10.1093/icesjms/fsy008

878 Maunder, M. N., & Punt, A. E. (2004). Standardizing catch and effort data: a review of recent
879 approaches. Fisheries Research, 70 , 141-159. doi:10.1016/j.fishres.2004.08.002.

880 Maunder, M. N., Thorson, J. T., Xu, H., Oliveros-Ramos, R., Hoyle, S. D., Tremblay-Boyer, L.,
881 Lee, H. H., Kai, M., Chang, S.-K., Kitakado, T., Albertsen, C. M., Minte-Vera, C. V.,
882 Lennert-Cody, C. E., Aires-da Silva, A. M., & Piner, K. R. (2020). The need for spatio-
883 temporal modeling to determine catch-per-unit effort based indices of abundance and
884 associated composition data for inclusion in stock assessment models. *Fisheries Research*,
885 229 , 105594. doi:10.1016/j.fishres.2020.105594.

886 Meyer, H., & Pebesma, E. (2021). Predicting into unknown space? Estimating the area of
887 applicability of spatial prediction models. *Methods in Ecology and Evolution*, 12, 1620-
888 1633. https://doi.org/10.1111/2041-210X.13650

889 Ming-An Lee, Jinn-Shing Weng, Kuo-Wei Lan, Ali Haghi Vayghan, Yi-Chen Wang & Jui-Wen
890 Chan. (2020). Empirical habitat suitability model for immature albacore tuna in the North

Pacific Ocean obtained using multisatellite remote sensing data. *International Journal of Remote Sensing*, 41(15), 5819-5837, doi: 10.1080/01431161.2019.1666317

Moore, C., Drazen, J. C., Radford, B. T., Kelley, C., & Newman, S. J. (2016). Improving essential fish habitat designation to support sustainable ecosystem-based fisheries management. Marine Policy, 69, 32-41. https://doi.org/10.1016/j.marpol.2016.03.021

Morley J. W., Selden R. L., Latour R. J., Frölicher T. L., Seagraves R. J., Pinsky M. L. (2018) Projecting shifts in thermal habitat for 686 species on the North American continental shelf. *PLoS ONE,* 13(5): e0196127. https://doi.org/10.1371/journal.pone.0196127

Muhling, B. A., Brodie, S., Smith, J. A., Tommasi, D., Gaitan, C. F., Hazen, E. L., Jacox, M. G., Auth, T. D. & Brodeur, R. D. (2020). Predictability of Species Distributions Deteriorates Under Novel Environmental Conditions in the California Current System. *Frontiers of Marine Science*, 7:589. doi: 10.3389/fmars.2020.00589

Nazzaro, L., Slesinger, E., Kohut, J., Saba, G. K., & Saba, V. S. (2021). Sensitivity of marine fish thermal habitat models to fishery data sources. Ecology and Evolution, 11(19):13001-13012. https://doi.org/10.1002/ece3.7817

Nye, J. A., Link, J. S., Hare, J. A., & Overholtz, W. J. (2009). Changing spatial distribution of fish stocks in relation to climate and population size on the Northeast United States continental shelf. *Marine Ecology Progress Series,* 393, 111-129. doi: 10.3354/meps08220

Pecl, G. T., Araújo, M. B., Bell, J. D., Blanchard, J., Bonebrake, T. C., Chen, I.-C., Clark, T. D., Colwell, R. K., Danielsen, F., Evengård, B., Falconi, L., Ferrier, S., Frusher, S., Garcia, R. A., Griffis, R. B., Hobday, A. J., Janion-Scheepers, C., Jarzyna, M. A., Jennings, S., … & Williams, S. E. (2017). Biodiversity redistribution under climate change: Impacts on ecosystems and human well-being. *Science*, 355(6332), eaai9214. https://doi.org/10.1126/science.aai9214

Pennino, M. G., Paradinas, I., Illian, J. B., Mu~noz, F., Bellido, J. M., Lopez-Qulez, A., & Conesa, D. (2019). Accounting for preferential sampling in species distribution models. *Ecology and Evolution*, 9, 653-663. doi:10.1002/ece3.4789.

Pinsky, M. L., Eikeset, A. M., McCauley, D. J., Payne, J. L., & Sunday, J. M. (2019). Greater vulnerability to warming of marine versus terrestrial ectotherms. *Nature*, 569(7754), 108-111.

Poloczanska, E. S., Brown, C. J., Sydeman, W. J., Kiessling, W., Schoeman, D. S., Moore, P. J., … & Richardson, A. J. (2013). Global imprint of climate change on marine life. Nat. Clim. Chang. 3, 919–925. doi: 10.1038/nclimate1958

Poloczanska E. S., Burrows M. T., Brown C. J., Molinos J. G., Halpern B. S., Hoegh-Guldberg O., Kappel C.V., Moore P. J., Richardson A. J., Schoeman D. S., & Sydeman W. J. (2016). Responses of marine organisms to climate change across oceans. *Frontiers in Marine Science*, 3(62).https://doi.org/10.3389/fmars.2016.00062

Pozo Buil, M., Jacox, M. G., Fiechter, J., Alexander, M. A., Bograd, S. J., Curchitser, E. N., Edwards, C. A., Rykaczewski, R. R., & Stock, C. A. (2021). A Dynamically Downscaled Ensemble of Future Projections for the California Current System. *Frontiers in Marine Science*, 8(324), https://doi.org/10.3389/fmars.2021.612874

R Core Team (2019). R: A language and environment for statistical computing. R Foundation for Statistical Computing, Vienna, Austria. URL https://www.R-project.org/.

Rogers, L. A., Griffin, R., Young, T., Fuller, E., St. Martin, K., & Pinsky, M. L. (2019). Shifting habitats expose fishing communities to risk under climate change. *Nature Climate Change*, 9(7), 512–516. https://doi.org/10.1038/s4155 8-019-0503-z

Rose, K.A., Fiechter, J., Curchitser, E. N., Hedstrom, K., … & Agostini, V. (2015). Demonstration of a fully-coupled end-to-end model for small pelagic fish using sardine and anchovy in the California Current. *Progress in Oceanography*, 138, 348-380

Rufener, M. C., Kristensen, K., Nielsen, J. R., Bastardie, F. (2021). Bridging the gap between commercial fisheries and survey data to model the spatiotemporal dynamics of marine species. *Ecological Applications*, N./a (2021), Article e02453, 10.1002/eap.2453(arXiv)

Sampson D.B. 1991 Fishing tactics and fish abundance, and their influence on catch rates, *ICES Journal of Marine Science*, 1991, vol. 48 (pg. 291-301)

Selden, R. L., Thorson, J. T., Samhouri, J. F., Bograd, S. J., Brodie, S., Carroll, G., Haltuch, M. A., Hazen, E. L., Holsman, K. K., Pinsky, M. L., Tolimieri, N., & Willis-Norton, E. (2019). Coupled changes in biomass and distribution drive trends in availability of fish stocks to US West Coast ports. *ICES Journal of Marine Science*, 77(1), 188–199. https://doi.org/10.1093/icesj ms/fsz211

Sequeira, A. M., Bouchet, P. J., Yates, K. L., Mengersen, K., & Caley, M. J. (2018). Transferring biodiversity models for conservation: opportunities and challenges. *Methods in Ecology and Evolution*, 9(5), 1250-1264.

Smith, J. A., Muhling, B., Sweeney, J., Tommasi, D., Pozo Buil, M., Fiechter, J., & Jacox, M. G. (2021a). The potential impact of a shifting Pacific sardine distribution on U.S. West Coast landings." *Fisheries Oceanography,* 30, 437-454, https://doi.org/10.1111/fog.12529

956 Smith, J. A., Tommasi, D., Welch, H., Hazen, E. L., Sweeney, J., Brodie, S., . . . & Jacox, M. G.
957 (2021b). Comparing Dynamic and Static Time-Area Closures for Bycatch Mitigation: A
958 Management Strategy Evaluation of a Swordfish Fishery. *Frontiers in Marine Science*,
959 8:630607. doi: 10.3389/fmars.2021.630607.

960 Smith, J. A., Pozo Buil M., Fiechter J., Tommasi, D., & Jacox, M. G. (2022) Projected novelty
961 in the climate envelope of the California Current at multiple spatial-temporal scales. *PLOS*
962 *Clim* 1(4): e0000022. https://doi.org/10.1371/journal.pclm.0000022

963 Smith, M. D., & Wilen, J. E. (2003). Economic impacts of marine reserves: the importance of
964 spatial behavior. *Journal of Environmental Economics and Management*, 46 , 183-206.
965 doi:10.1016/s0095-0696(03)00024-x.

966 Sorte, C.J., Williams, S.L., & Carlton, J.T. (2010). Marine range shifts and species
967 introductions: comparative spread rates and community impacts. *Global Ecology and*
968 *Biogeography*. 19, 303–316. https://doi.org/10.1111/j.1466-8238.2009.00519.x

969 Steen, V., Sofaer, H. R., Skagen, S. K., Ray, A. J., & Noon, B. R. (2017). Projecting species'
970 vulnerability to climate change: which uncertainty sources matter most and extrapolate
971 best?. *Ecology and Evolution*, 7(21), 8841-8851. doi: 10.1002/ece3.3403

972 Stephens, A., & MacCall, A., (2004). A multispecies approach to subsetting logbook data for
973 purposes of estimating CPUE. *Fisheries Research*. 70, 299-310.
974 https://doi.org/10.1016/j.fishres.2004.08.009

975 St. Martin, K., & Hall-Arber, M. (2008a). The missing layer: geo-technologies, communities,
976 and implications for marine spatial planning. Marine Policy, 32: 779–786.

977 Støa, B., Halvorsen, R., Mazzoni, S., & Gusarov, V. I. (2018). Sampling bias in presence-only
978 data used for species distribution modelling: Theory and methods for detecting sample bias
979 and its effects on models. *Sommerfeltia*, 38, 1–53. https://doi.org/10.2478/som-2018-0001

980 Sumaila, U. R., Palacios-Abrantes, J., & Cheung, W. W. L. (2020). Climate change, shifting
981 threat points, and the management of transboundary fish stocks. *Ecology and Society*
982 25(4):40. https://doi.org/10.5751/ES-11660-250440

983 Tessarolo, G., Rangel, T. F., Araujo, M. B., & Hortal, J. (2014). Uncertainty associated with
984 survey design in species distribution models. *Diversity and Distributions*, 20, 1258– 1269.
985 https://doi.org/10.1111/ddi.12236

986 Thuiller W, Brotons L, Araújo MB *et al*. (2004) Effects of restricting environmental range of
987 data to project current and future species distributions. *Ecography*, 27, 165– 172.DOI:
988 10.1111/j.0906-7590.2004.03673.x

Urbisci, L.C., Stohs, S.M. & Piner, K.R. From sunrise to sunset in the California Drift Gillnet Fishery: an examination of the effects of time and area closures on the catch and catch rates of pelagic species. *Marine Fisheries Review* 78, 1-11 (2016).

van Putten, I.E. et al. Theories and behavioural drivers underlying fleet dynamics models. *Fish and Fisheries* 13, 216-235 (2012)

Veneziani, M., Edwards, C.A., Doyle, J.D., & Foley, D. (2009) A central California coastal ocean modeling study: 1. Forward model and the influence of realistic versus climatological forcing. *Journal of Geophysical Research: Oceans* 114(C4). doi:10.1029/2008jc004774

Wilen, J. E. (2004). Spatial Management of Fisheries. *Marine Resource Economics*, 19 , 7-19.

Wood, S. N. 2017. Generalized additive models: an introduction with R. – CRC Press.

Yao, Y., A. Vehtari, D. Simpson, and A. Gelman. (2018). Using stacking to average Bayesian predictive distributions (with discussion). *Bayesian Analysis* 13(3): 917-1007.

Yates, K. L., Bouchet, P. J., Caley, M. J., Mengersen, K., Randin, C. F., Parnell, S., ... & Sequeira, A. M. (2018). Outstanding challenges in the transferability of ecological models. *Trends in ecology & evolution*, 33(10), 790-802.

Zurell, D., Elith, J., & Schröder, B. (2012). Predicting to new environments: tools for visualizing model behaviour and impacts on mapped distributions. *Diversity and Distributions*, 18(6), 628-634.

TABLES AND FIGURES

Table 1: Model fit and performance (AUC, RMSE, COR), climatic bias during historical training period 1985-2010 for all environmental parameters and sampling scenarios, and the proportion of the ROMS sampling domain covered by each sampling scenario.

Sampling Scenario	AUC (P)		RMSE		COR		Measures of Climatic Bias						Proportion area covered
							SST		Chlorophyl		MLD		
	GAMs	BRTs	GAMs	BRTs	GAMs	BRTs	HD	Cohen's d	HD	Cohen's d	HD	Cohen's d	
Random	0.92	0.92	5.09	5.10	0.77	0.77	0.03	-0.07	0.05	0.06	0.03	-0.03	89.80%
Preferential	0.91	0.90	5.10	5.39	0.77	0.75	0.41	-0.41	0.23	-0.20	0.17	0.05	50.18%
Port Southern Offshore	0.84	0.77	6.60	8.85	0.72	0.55	0.51	-0.71	0.29	-0.32	0.26	0.39	11.55%
Port Southern Nearshore	0.54	0.78	8.06	10.61	0.69	0.46	0.55	-0.97	0.32	-0.18	0.43	0.87	7.97%
Port Northern Offshore	0.89	0.86	5.84	6.78	0.72	0.65	0.50	0.47	0.36	-0.45	0.25	0.23	27.25%
Port Northern Nearshore	0.90	0.85	5.67	6.31	0.74	0.67	0.54	0.73	0.40	-0.50	0.35	0.55	20.28%
Port Middle Offshore	0.91	0.88	5.15	5.61	0.76	0.72	0.47	-0.22	0.30	-0.42	0.21	0.08	24.70%
Port Middle Nearshore	0.89	0.87	5.47	5.84	0.74	0.71	0.49	0.07	0.45	-0.85	0.25	0.21	12.11%
Port All Offshore	0.91	0.90	5.12	5.37	0.77	0.75	0.40	-0.40	0.28	-0.35	0.20	0.19	30.17%
Port All Nearshore	0.90	0.87	5.48	5.94	0.75	0.71	0.33	-0.17	0.37	-0.68	0.23	0.40	23.37%
Closed Area Small	0.91	0.89	5.09	5.44	0.77	0.74	0.41	-0.46	0.23	-0.17	0.16	0.07	48.35%
Closed Area Medium	0.91	0.90	5.07	5.26	0.77	0.75	0.42	-0.52	0.23	-0.10	0.16	0.06	40.70%
Closed Area Large	0.91	0.90	5.13	5.31	0.77	0.75	0.44	-0.61	0.24	-0.07	0.16	0.12	33.88%
Bycatch	0.91	0.90	5.23	5.42	0.77	0.75	0.37	-0.40	0.23	0.04	0.16	-0.12	52.53%

Table 2: Hellinger distance (HD) for all environmental parameters, sampling scenarios, and future time periods. The HD for the future periods provides an indication of the novelty of the environments during those future periods relative to the environment conditions captured by each sampling scenario during the historical period. Greener colors represent low climate novelty while redder colors represent greater climate novelty when comparing the environmental conditions sampled in the historical period to the future period.

	Early Century: 2011:2039			Mid Century: 2040-2069			Late Century: 2070-2100		
Sampling Scenario	Temp	MLD	Chl	Temp	MLD	Chl	Temp	MLD	Chl
Random	0.16	0.07	0.06	0.36	0.08	0.09	0.54	0.12	0.18
Preferential	0.38	0.15	0.24	0.42	0.18	0.29	0.54	0.19	0.36
Port Southern Offshore	0.48	0.24	0.30	0.46	0.23	0.36	0.50	0.20	0.43
Port Southern Nearshore	0.51	0.42	0.32	0.49	0.38	0.37	0.49	0.35	0.43
Port Northern Offshore	0.53	0.23	0.38	0.67	0.24	0.43	0.84	0.23	0.51
Port Northern Nearshore	0.60	0.34	0.42	0.75	0.31	0.48	0.90	0.29	0.56
Port Middle Offshore	0.46	0.19	0.32	0.49	0.21	0.37	0.63	0.22	0.45
Port Middle Nearshore	0.48	0.23	0.48	0.56	0.24	0.53	0.73	0.23	0.60
Port All Offshore	0.37	0.18	0.30	0.41	0.19	0.36	0.54	0.18	0.44
Port All Nearshore	0.28	0.21	0.41	0.39	0.19	0.45	0.58	0.17	0.53
Closed Area Small	0.39	0.14	0.24	0.42	0.16	0.29	0.53	0.16	0.36
Closed Area Medium	0.39	0.14	0.23	0.41	0.17	0.28	0.51	0.17	0.34
Closed Area Large	0.42	0.14	0.24	0.44	0.16	0.28	0.51	0.16	0.34
Bycatch	0.34	0.16	0.21	0.40	0.19	0.23	0.54	0.21	0.27

Table 3: Root mean squared error (RMSE) of modeled and 'true' biomass, by time period and sampling scenario. Greener colors reflect lower errors, redder colors reflect higher errors.

Sampling Scenario	2011-2039		2040-2069		2070-2100	
	GAM	BRT	GAM	BRT	GAM	BRT
Random	5.47	5.50	5.55	5.52	5.50	5.30
Preferential	5.61	5.79	6.56	6.25	8.15	6.56
Port Southern Offshore	6.47	7.50	6.60	6.39	7.35	6.09
Port Southern Nearshore	7.46	8.85	7.26	7.07	8.05	6.37
Port Northern Offshore	7.29	7.31	9.73	7.89	12.59	8.24
Port Northern Nearshore	6.67	6.84	8.24	7.12	9.98	7.02
Port Middle Offshore	5.61	5.78	5.97	5.97	6.49	6.08
Port Middle Nearshore	6.47	6.27	7.97	6.72	9.69	7.11
Port All Offshore	5.67	5.69	6.28	5.98	6.99	6.28
Port All Nearshore	6.26	6.17	7.28	6.30	8.41	6.39
Closed Area Small	5.62	5.68	6.40	5.88	7.39	5.98
Closed Area Medium	5.55	5.57	6.23	5.79	7.16	5.92
Closed Area Large	5.61	5.63	6.45	5.94	7.64	6.03
Bycatch	5.84	5.81	6.99	6.25	8.60	6.57

FIGURE CAPTIONS:

Figure 1. Map of the study area, showing the entire ROMS domain. The black outline off the coast of California (CA), Oregon (OR), and Washington (WA) indicates the United States Exclusive Economic Zone (EEZ). The ports used for the distance from port sampling scenarios are labeled and indicated with black squares on the map.

Figure 2. Flow diagram illustrating the 4 main steps of the simulation process.

Figure 3: Maps and time-series of dynamically downscaled environmental covariates projected to 2100. Maps show the average historical spring conditions for the dynamically downscaled environmental and biological covariates used in the operating model and/or the estimation models (mixed layer depth, SST, zooplankton, prey abundance, and chl surface), and distribution of the simulated species biomass (kg) from 1985-2010. The time-series plots show the spatially aggregated average annual spring conditions for the entire simulation time period (1985-2100). The red vertical line at 2010 indicates the beginning of the forecast period, and the red vertical line at 2070 indicates beginning of the late-century period. The dashed lines represent the mean +/- 1 SD.

Figure 4: Sampling locations for each sampling scenario during the training period 1985-2010 used to fit the estimation models. The black dots indicate the locations of the ports used for the distance from ports scenarios. The percentages shown in each facet indicate the percentage of the ROMS domain covered by each sampling scenario based on the area of a concave hull around each set of sampling points.

Figure 5: Physical Climate Bias (top row) and Climate Novelty (bottom three rows) as a function of Sampling Scenario. Difference in mean value (Cohen's D) versus difference in the sampling distribution compared to the distribution of the environmental conditions across the entire domain (Hellinger distance). Sampling data with a distribution of climate values identical to the climate values across the domain would be located at (0, 0). The size of each point is scaled by the RMSE each time period averaged over the GAM and BRT models for each sampling scenario. Negative values of Cohen's D (to the right of the vertical line at x=0) indicate that the mean value for a parameter is greater in the sampling scenario compared to the full domain. The horizontal line at y=0.5 indicates the threshold for novelty.

Figure 6: Biomass time series for 1985-2100 showing the true biomass, each of the 14 scenarios for the GAMs and BRTs (a) and the difference between the true biomass and biomass predicted with each of the scenarios across the time series (b).

Figure 7: Latitudinal center of gravity time series for 1985-2100 showing the latitudinal center of gravity, each of the 14 scenarios for the GAMs and BRTs (a) and the difference between the

1110 true center of gravity and center of gravity predicted with each of the scenarios across the time
1111 series (b).
1112
1113 **Figure 8:** Maps of difference in the predicted species distribution averaged across the historical
1114 period (1985-2010; top panel) and each of the future periods (2011-2039, 2040-2069, and 2070-
1115 2100). Here we show the spatial differences between the predicted distributions from two
1116 sampling scenarios with low climate bias, the random and preferential sampling, and three
1117 sampling scenarios with high climate bias, ports southern nearshore, ports middle nearshore, and
1118 ports northern nearshore, fit with a GAM, compared with the true simulated distribution. See
1119 Figs. S19-S22 to see spatial differences for all sampling scenarios. Red areas indicate areas
1120 where the model overpredicts the biomass, and blue areas where the model underpredicts the
1121 biomass.

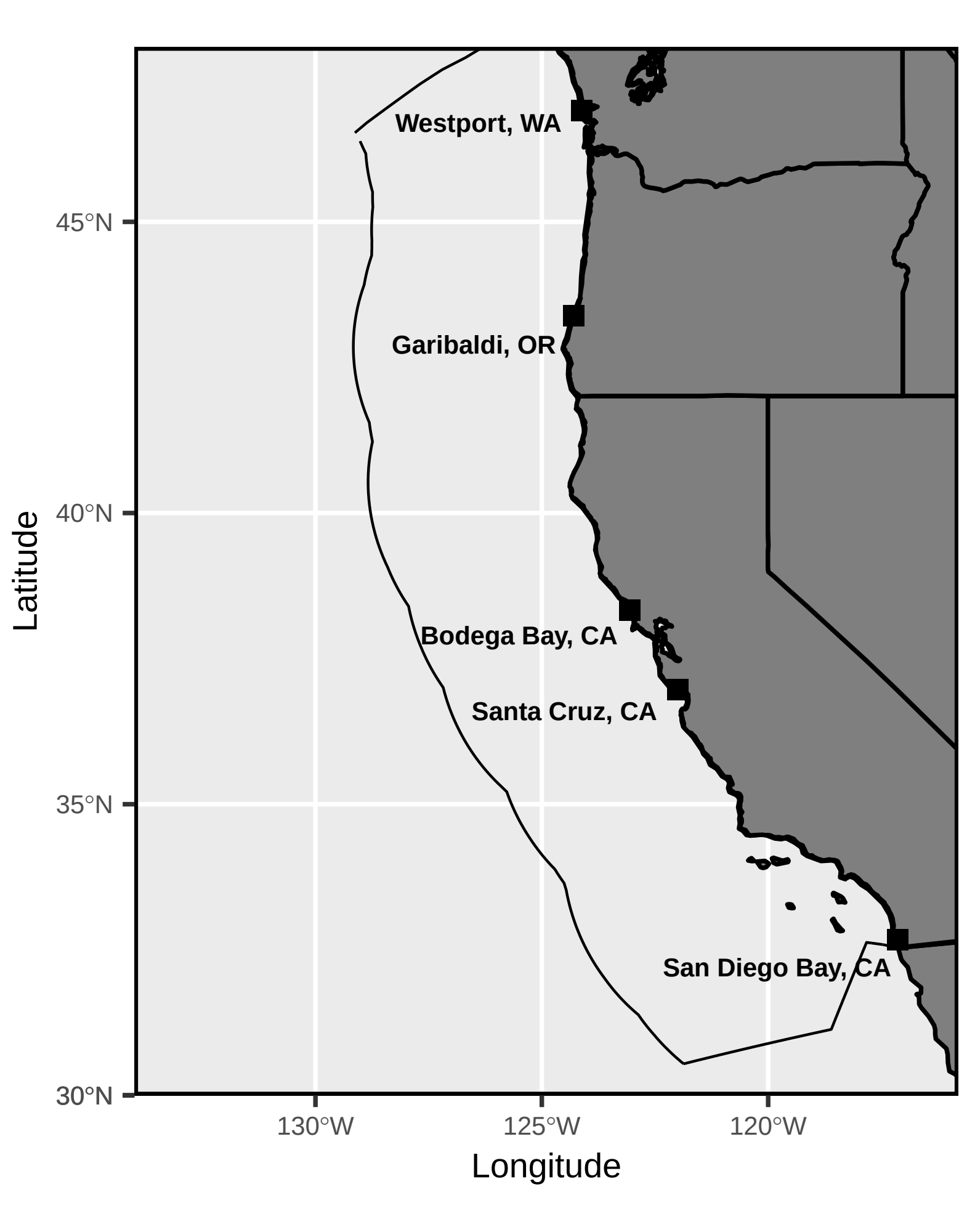
Westport, WA
Garibaldi, OR
Bodega Bay, CA
Santa Cruz, CA
San Diego Bay, CA
45°N
40°N
35°N
30°N
130°W
125°W
120°W
Latitude
Longitude

Step 1:
Creating virtual species true distribution

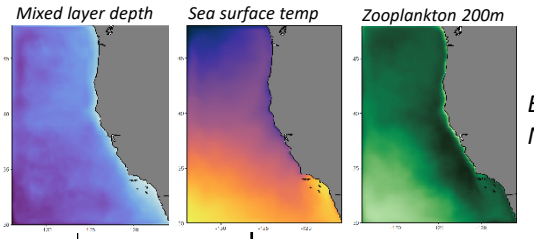

Environmental Datasets from NEMUCSC-ROMS

Generate virtual species distribution according to a linear model of the environmental variables

True center of gravity

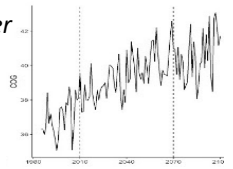

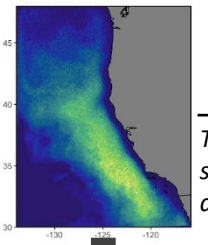

True virtual species distribution

Step 2:
Sampling virtual species distribution with simulated fishery-dependent bias

Sampling (n = 100)

Random Sampling

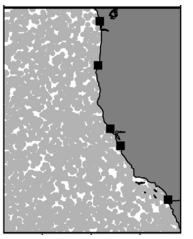

Preferential Sampling

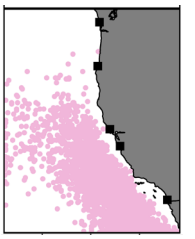

Bycatch Avoidance

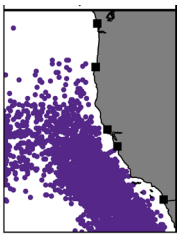

Closed Area

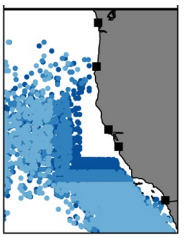

Distance from Port

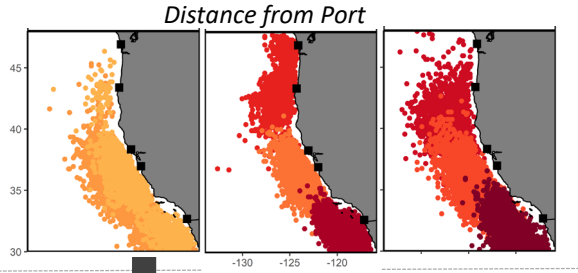

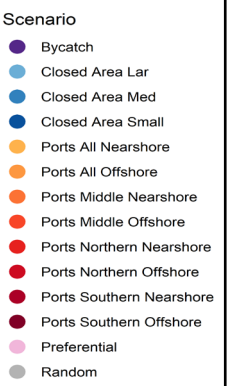

SDMs — **GAM** | **BRT**

Step 3:
Fit SDMs to simulated data

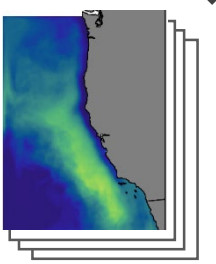

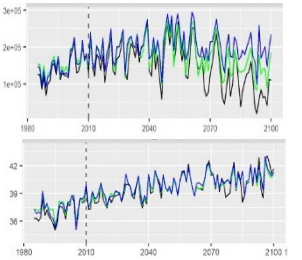

Step 4:
Model performance and evaluation

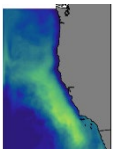

compare

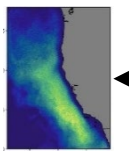

<u>Evaluation metrics</u>
RMSE | AUC | Hellinger's distance | Cohen's D

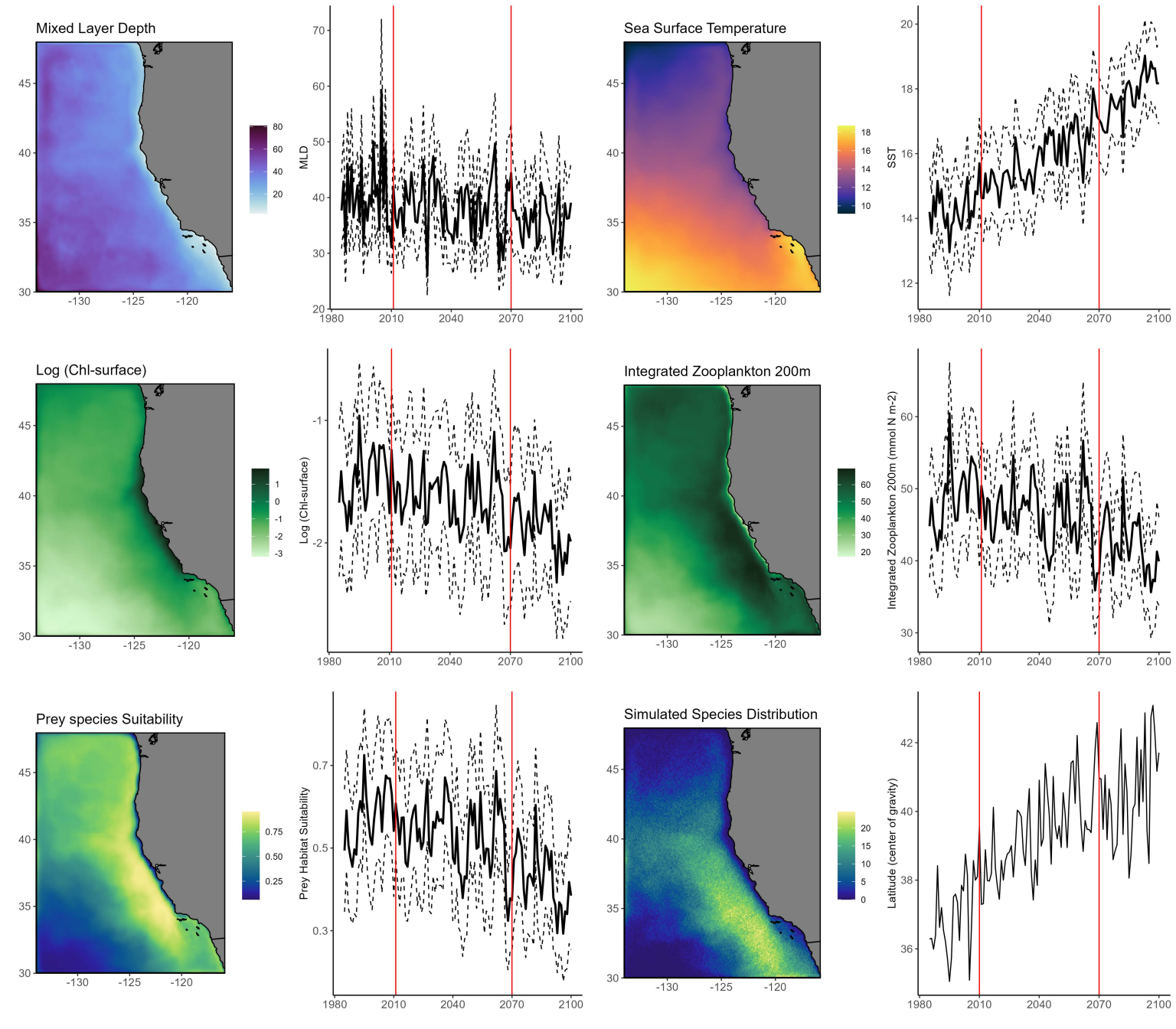
Mixed Layer Depth
MLD
Sea Surface Temperature
SST
Log (Chl-surface)
Log (Chl-surface)
Integrated Zooplankton 200m
Integrated Zooplankton 200m (mmol N m-2)
Prey species Suitability
Prey Habitat Suitability
Simulated Species Distribution
Latitude (center of gravity)
1980
2010
2040
2070
2100
-130
-125
-120

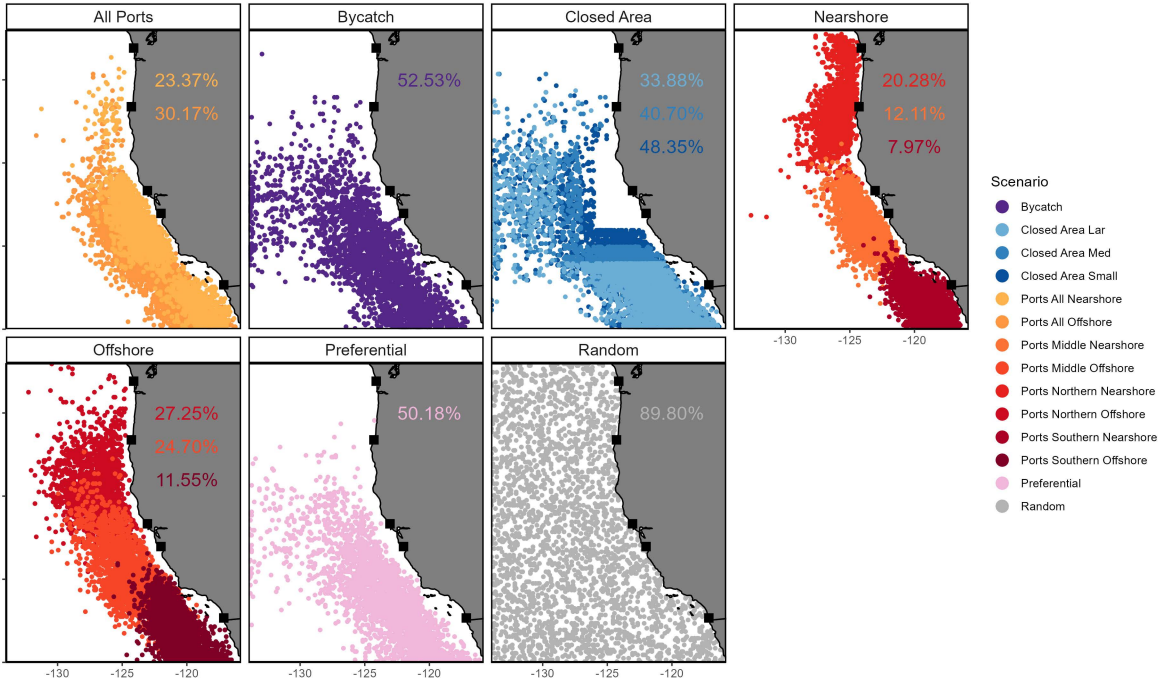
All Ports
23.37%
30.17%
Bycatch
52.53%
Closed Area
33.88%
40.70%
48.35%
Nearshore
20.28%
12.11%
7.97%
Offshore
27.25%
24.70%
11.55%
Preferential
50.18%
Random
89.80%
45
40
35
30
-130
-125
-120
Scenario
Bycatch
Closed Area Lar
Closed Area Med
Closed Area Small
Ports All Nearshore
Ports All Offshore
Ports Middle Nearshore
Ports Middle Offshore
Ports Northern Nearshore
Ports Northern Offshore
Ports Southern Nearshore
Ports Southern Offshore
Preferential
Random

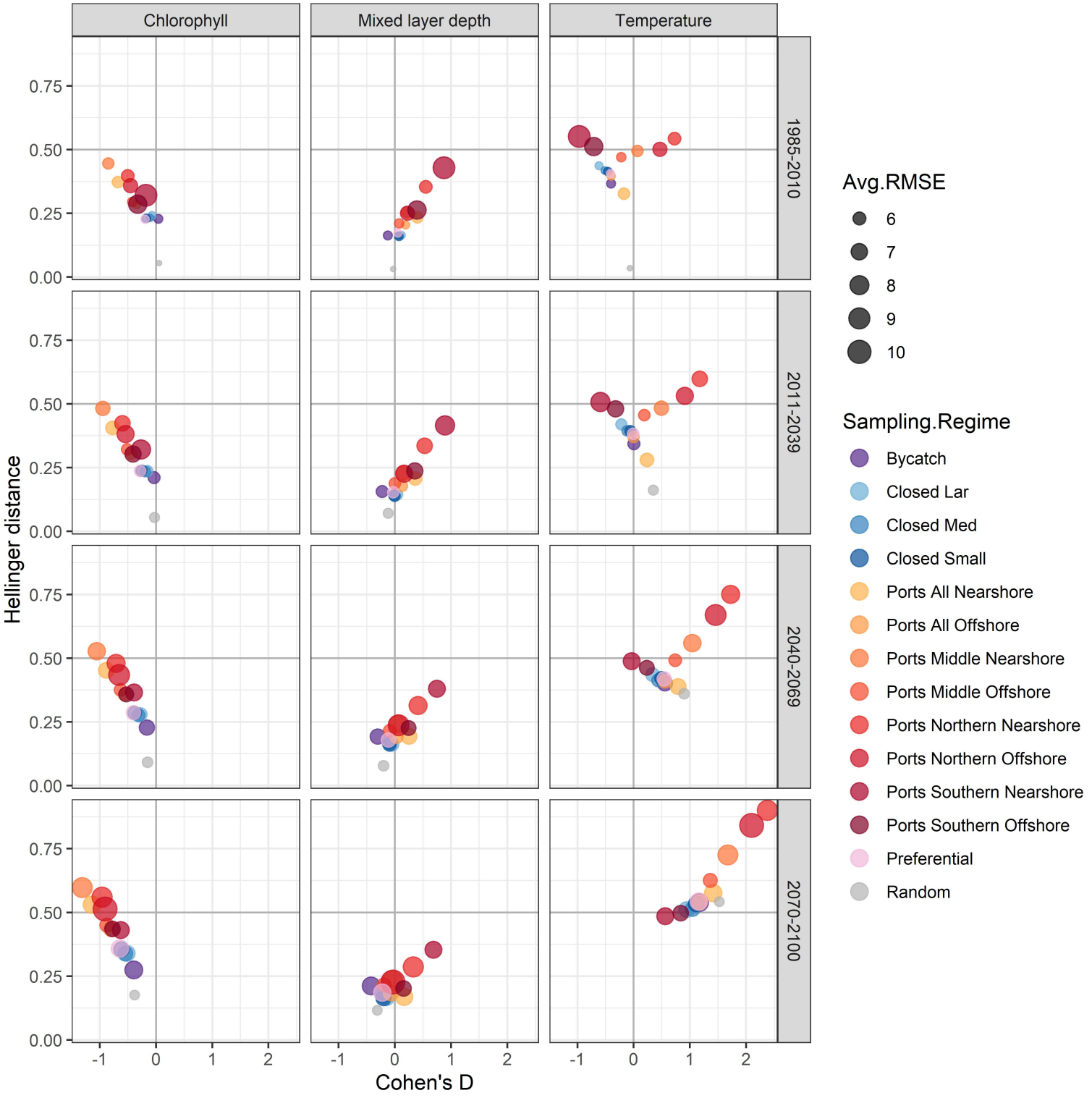
Chlorophyll
Mixed layer depth
Temperature
1985-2010
2011-2039
2040-2069
2070-2100
Hellinger distance
0.00
0.25
0.50
0.75
Cohen's D
-1
0
1
2
Avg.RMSE
6
7
8
9
10
Sampling.Regime
Bycatch
Closed Lar
Closed Med
Closed Small
Ports All Nearshore
Ports All Offshore
Ports Middle Nearshore
Ports Middle Offshore
Ports Northern Nearshore
Ports Northern Offshore
Ports Southern Nearshore
Ports Southern Offshore
Preferential
Random

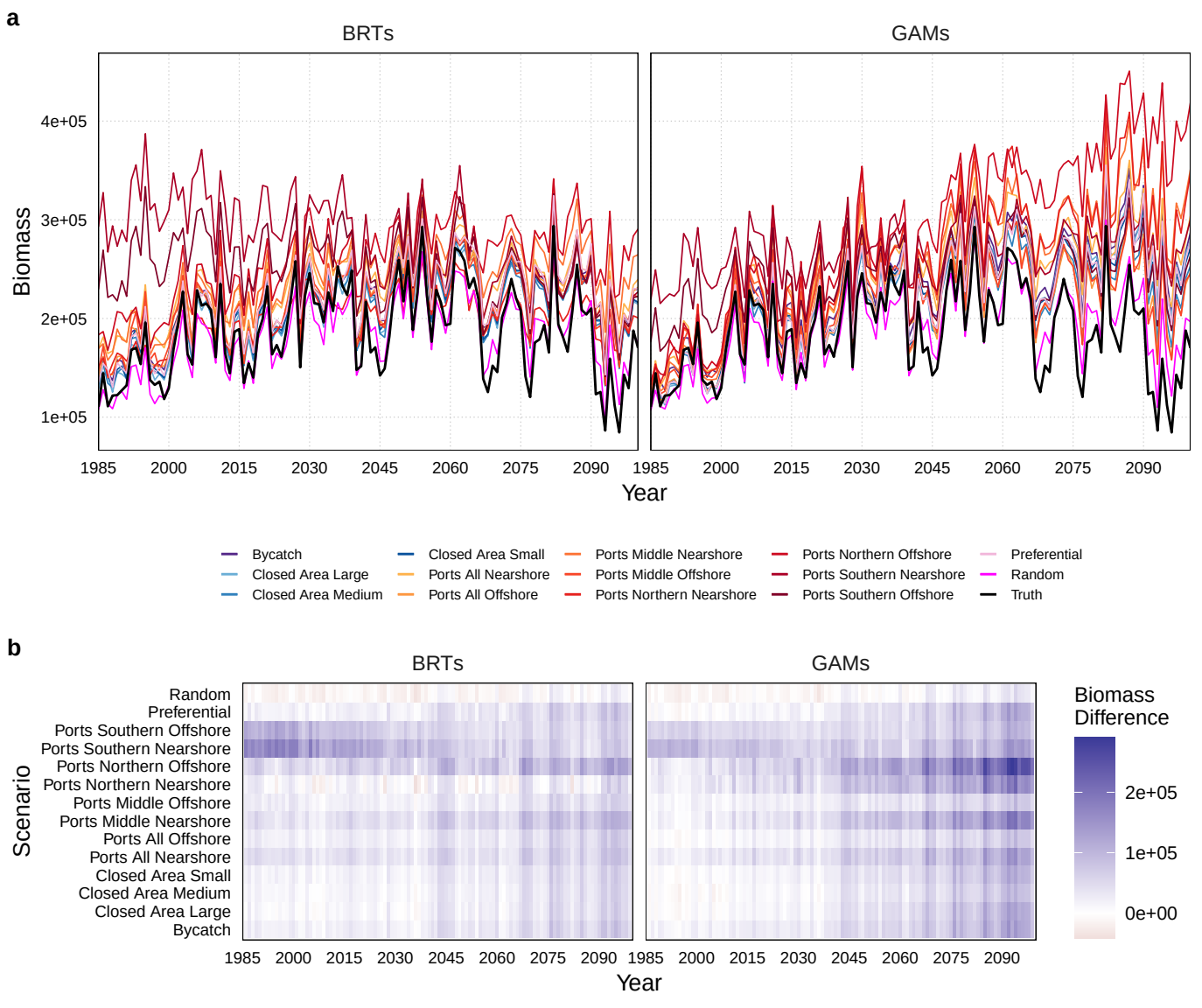
a
BRTs
GAMs
Biomass
4e+05
3e+05
2e+05
1e+05
1985
2000
2015
2030
2045
2060
2075
2090
Year
Bycatch
Closed Area Large
Closed Area Medium
Closed Area Small
Ports All Nearshore
Ports All Offshore
Ports Middle Nearshore
Ports Middle Offshore
Ports Northern Nearshore
Ports Northern Offshore
Ports Southern Nearshore
Ports Southern Offshore
Preferential
Random
Truth
b
BRTs
GAMs
Scenario
Random
Preferential
Ports Southern Offshore
Ports Southern Nearshore
Ports Northern Offshore
Ports Northern Nearshore
Ports Middle Offshore
Ports Middle Nearshore
Ports All Offshore
Ports All Nearshore
Closed Area Small
Closed Area Medium
Closed Area Large
Bycatch
Year
Biomass Difference
2e+05
1e+05
0e+00

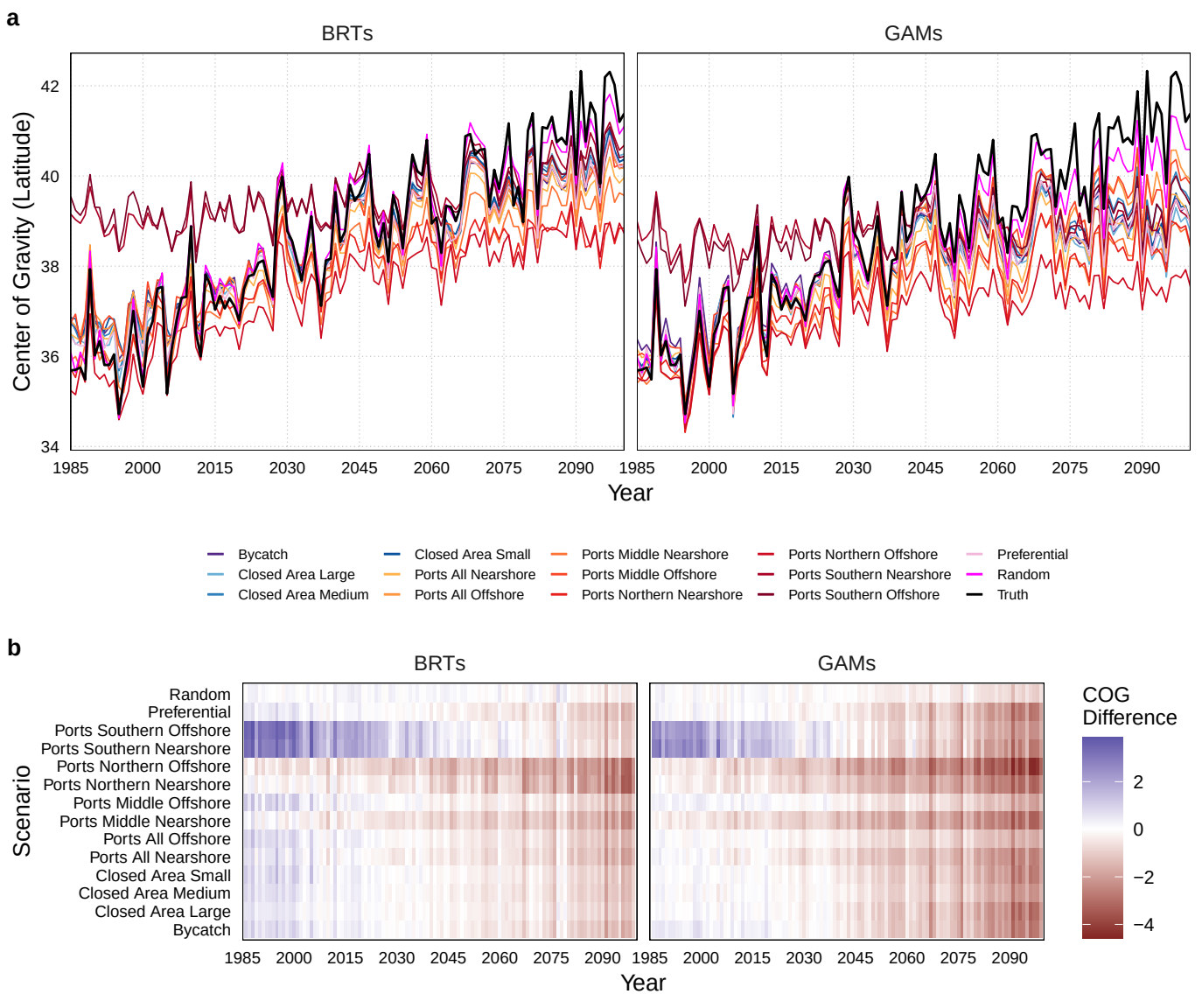
a
BRTs
GAMs
Center of Gravity (Latitude)
42
40
38
36
34
1985
2000
2015
2030
2045
2060
2075
2090
Year
Bycatch
Closed Area Large
Closed Area Medium
Closed Area Small
Ports All Nearshore
Ports All Offshore
Ports Middle Nearshore
Ports Middle Offshore
Ports Northern Nearshore
Ports Northern Offshore
Ports Southern Nearshore
Ports Southern Offshore
Preferential
Random
Truth
b
BRTs
GAMs
Scenario
Random
Preferential
Ports Southern Offshore
Ports Southern Nearshore
Ports Northern Offshore
Ports Northern Nearshore
Ports Middle Offshore
Ports Middle Nearshore
Ports All Offshore
Ports All Nearshore
Closed Area Small
Closed Area Medium
Closed Area Large
Bycatch
Year
COG Difference
2
0
−2
−4

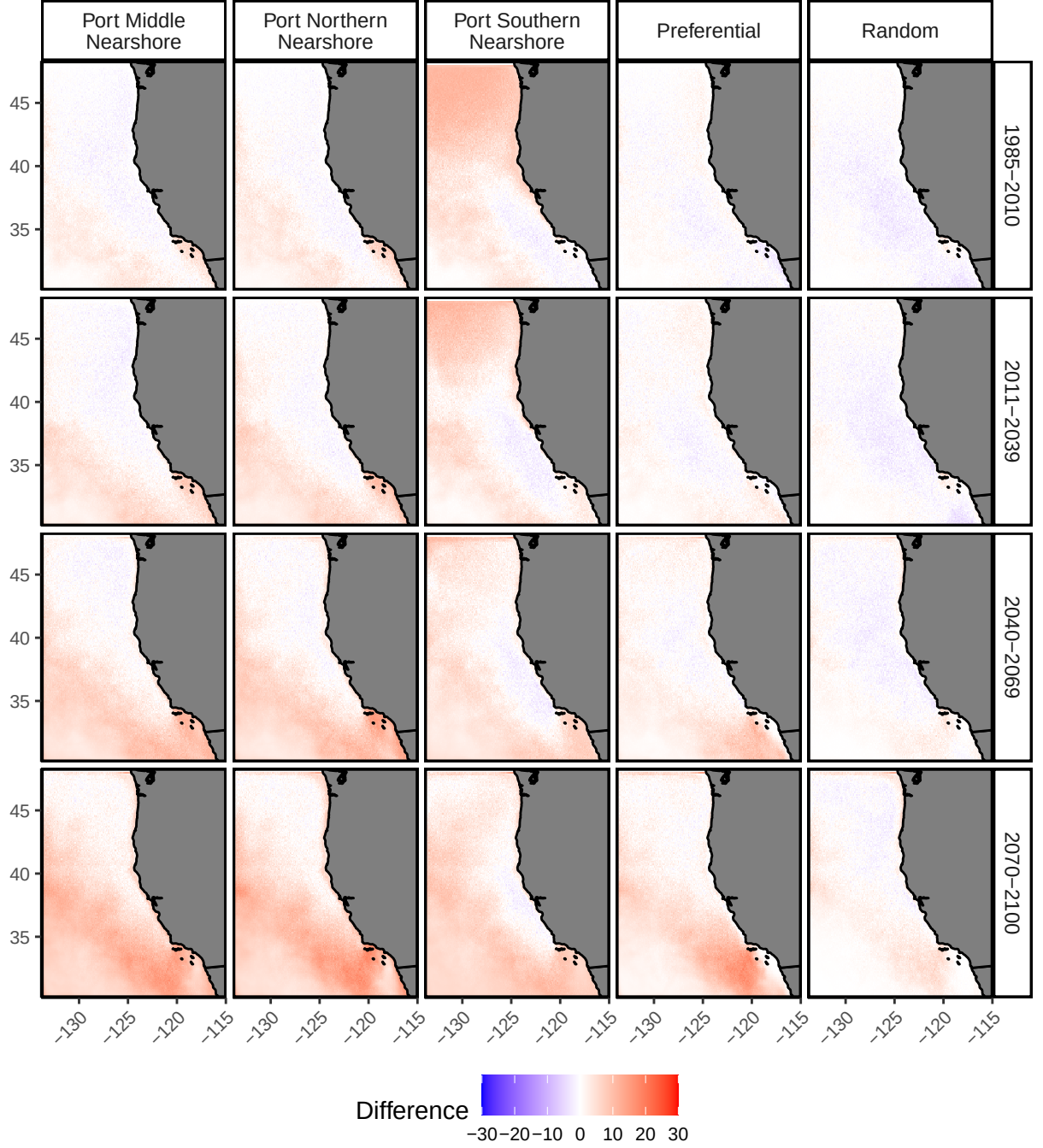
Port Middle Nearshore
Port Northern Nearshore
Port Southern Nearshore
Preferential
Random
1985–2010
2011–2039
2040–2069
2070–2100
45
40
35
−130
−125
−120
−115
Difference
−30 −20 −10 0 10 20 30

Supplementary Materials

S1: Supplemental Methods

Sampling Process: simulating fishery-dependent data collection

For the *Preferential* sampling scenario, the fishing suitability raster resulted from a positive logistic function of the habitat suitability of the target species in the previous year (y-1). We used the y-1 suitability as fishermen often base their choice of where to fish on where they found the fish in the previous year (Sampson 1991). Therefore, we are using the habitat suitability in the previous year as a proxy of where the fishermen were likely to find the fish in the previous year for this analysis. We built the fishing suitability raster using beta βs (inflection points) for the logistic function of 0.7.

For the *Port* scenarios, fishing suitability was a function of a positive logistic response to target species habitat suitability in the previous year, with a beta=0.7, and a negative logistic response to distance from port. We built fishing suitability rasters for 8 different distance from port scenarios. Two scenarios simulated situations where fishermen were limited to fishing around northern ports in Washington (Westport, WA -124.114934, 46.911534) and Oregon (Garibaldi, OR, -124.292000, 43.383975), two scenarios simulated fishermen being limited to fishing around ports within the middle of the ROMS domain (Santa Cruz, CA (-122.001620, 36.965719), and Bodega Bay, CA (-123.050618, 38.334302)), two scenarios simulated fishing limited to fishing around a port in southern CA (San Diego Bay, CA (-117.1441, 32.6717)), and two scenarios included all ports. One of the scenarios for each port simulated an offshore fishery where fishing suitability was high up until about 300 miles from a port, and one scenario simulated a nearshore fishery where fishing suitability declines after about 50 miles from a port. The distance from each port to every cell in the raster was calculated using *distanceFromPoints* function in R. For the scenarios where more than one port was used, the lesser distance of each cell to the ports was used.

For the *Bycatch* scenario, we simulated the distribution of a turtle-like bycatch species which we used to impact fishing location suitability. The simulated bycatch species preferred warmer temperatures than our target species, exhibiting a unimodal response to SST (mean=25,

sd=10), and similar to the simulated prey species of our target species exhibited a positive logistic response to zooplankton abundance. The fishing location suitability was determined by a positive logistic function of target species habitat suitability in the previous year (with beta=0.7), and a negative logistic function of the bycatch species habitat suitability in the current year. This simulates a situation where fishermen actively avoid fishing in areas of high bycatch risk (high habitat suitability for bycatch species) but are still also attempting to fish in areas that have good habitat suitability for their target species (Smith et al. 2021, Hazen et al. 2018, Howell et al. 2008).

For the *Closed Area* scenario, fishing suitability was determined by multiplying the fishing suitability raster developed for the *Preferential* scenario with a beta=0.7 by a raster of 0s and 1s, where 0 values were for cells within the closed area. This effectively made it so cells within the closed area had a 0% chance of being sampled. We simulated fishing locations based on three different sizes of the closed area. The smallest closed area was a box with its corners at longitude and latitudes of -126, -118, 36, 41. The medium sized closed area had corners at -127, -118, 35, 42, and the largest closed area at -129, -118, 34, 43. The largest closed area was similar in size and location to the seasonally closed Pacific Leatherback Conservation Area (PLCA) off the US west coast; the PLCA is intended to reduce incidental bycatch of endangered leatherback turtles (*Dermochelys coriacea*) (Urbisci et al 2016).

Assessment of Climatic Bias in the Sampling Scenarios

We used two different metrics to obtain climatic bias and novelty, Cohen's d and Hellinger Distance (HD). Cohen's d is a measure of the difference between the means of two groups, and we calculated this using the below formula:

$$\mathrm{d} = \frac{(M1 - M2)}{Pooled\ SD}$$

Where M1 is the mean of the first sampling regime (e.g. SST in the partially sampled historical climate), and M2 is the mean for the second sampling regime being compared (e.g. SST in the full historical or future climate used for prediction), and the denominator is the pooled standard deviation. A value of d = 0.2 is generally considered a small difference or effect, 0.5 a medium, and 0.8 a large difference (Cohen 1988). The Hellinger distance is a measure of the difference

between two probability distributions (see Legendre & Legendre 2012) and we calculate this using the below formula for each environmental parameter:

$$H(P, Q) = \frac{1}{\sqrt{2}} \sqrt{\sum_{i=1}^{k} (\sqrt{p_i} - \sqrt{q_i})^2}$$

Where p_i is the probability distribution of the environmental parameter of interest in the entire sampling domain and q_i is the probability distribution for that same environmental parameter for a particular sampling scenario. The HD measures how much information is contained in one distribution relative to another. With this metric the two distributions being compared become more similar as the difference in the proportion of sites at each value of the environmental covariate declines. HD values >0.5 have been proposed as a threshold of novelty, where the distributions become more dissimilar than they are similar (Johnson and Watson et al *in prep*).

Table S1: Variable used to simulate species spatially explicit distribution and fishery-dependent sampling scenario suitability rasters. μ is the mean and σ the standard deviation for the normal response curves. For the logistic response curves, α is the scale parameter which controls the slope of the curve (the growth rate), and β is the location parameter specifying the time when curve reaches the midpoint of the growth/decline trajectory.

Suitability Raster	Variable	Description	Parameter 1	Parameter 2	Distribution
HMS species archetype	SST	Sea surface temperature	μ = 17	σ = 4	normal
	MLD	Mid-layer depth	μ = 50	σ = 30	normal
	Prey presence	Preference for prey	α = -0.15	β = 0.4	logistic
	Biomass (kg)	Biomass if the species is present in a grid cell	log μ = 3.29	log (σ) = 0.26	Log normal
	Occurrence (0 or 1)	Occurrence as a function of habitat suitability	α = -0.07	β = 0.4	logistic
Prey species	SST	Sea surface temperature	μ = 14	σ = 7	normal
	zoo_200m	Zooplankton integrated over top 50m	α = -10	β = 45	logistic
Bycatch species	SST	Sea surface temperature	μ = 25	σ = 10	normal
	zoo_200m	Zooplankton integrated over top 50m	α = -6	β = 50	logistic
Preferential	HMS species presence t-1	HMS habitat suitability in the previous year	α = -0.05	β = 0.7	logistic
Distance - Nearshore scenarios	HMS species presence t-1	HMS habitat suitability in the previous year	α = -0.05	β = 0.7	logistic
	max distance	Controls how suitability declines in relation to distance from port	α = 50	β = 110	logistic
Distance - Offshore scenarios	HMS species presence t-1	HMS habitat suitability in the previous year	α = -0.05	β = 0.7	logistic
	max distance	Controls how suitability declines in relation to distance from port	α = 50	β = 480	logistic
Bycatch avoidance	HMS species presence t-1	HMS habitat suitability in the previous year	α = -0.05	β = 0.7	logistic
	Bycatch species presence	Habitat suitability of a simulated bycatch species	α = 0.05	β = 0.5	logistic

Table S2: Model formulation for the GAMs and BRTs fitted in the simulation

Model	Description	Model Component	R syntax
GAM_E	environmental covariates only	Pr(presence)	s(SST)+ s(MLD) + s(chl); family = binomial
		log(biomass)	s(SST)+ s(MLD) + s(chl); family = gaussian
GAM_E+ST	environmental covariates and spatiotemporal covariates	Pr(presence)	(SST) + s(MLD) + s(chl) + te(lat, lon, year, d=c(2,1), bs=c('ds','tp'), m=(c(1,.5),1), k=c(30,10))
		log(biomass)	(SST) + s(MLD) + s(chl) + te(lat, lon, year, d=c(2,1), bs=c('ds','tp'), m=(c(1,.5),1), k=c(30,10))
BRT_E	environmental covariates only	Pr(presence)	gbm.x = c(SST, MLD, chl-surface) gbm.y = 'pres', family = "bernoulli", tree.complexity = 3, learning.rate = 0.01, bag.fraction = 0.6
		log(biomass)	gbm.x = c(SST, MLD, chl-surface) gbm.y = 'log(biomass)', family = "gaussian", tree.complexity = 3, learning.rate = 0.01, bag.fraction = 0.6,
BRT_E+ST	environmental covariates and spatiotemporal covariates	Pr(presence)	gbm.x = c(SST, MLD, chl-surface, lat, long, year) gbm.y = 'pres', family = "bernoulli", tree.complexity = 3, learning.rate = 0.01, bag.fraction = 0.6
		log(biomass)	gbm.x = c(SST, MLD, chl-surface, lat, lon, year) gbm.y = 'log(biomass)', family = "gaussian", tree.complexity = 3, learning.rate = 0.01, bag.fraction = 0.6

Table S3: Deviance explained for the presence and abundance components of the GAMs and BRTs models for both those with only environmental covariates and the ones which included both environmental and space-time covariates.

Scenario	Presence Component				Abundance Component			
	Environment Only		Env + Spacetime		Environment Only		Env + Spacetime	
	GAM	BRT	GAM	BRT	GAM	BRT	GAM	BRT
Bycatch	45	49.8	51.7	51.4	35	41	38.7	44.1
Closed Area Large	53.1	57.4	60	62.9	37.7	40.8	37.7	42.3
Closed Area Medium	49.9	54.8	53.1	57	36.6	41.4	38.9	45
Closed Area Small	48.9	54.1	50.1	58.7	30.5	34.6	33.5	35.2
Port All Nearshore	27.3	36	27.4	31.7	29.6	33.9	30.3	34
Port All Offshore	41.4	47.3	46	48	28.1	33.7	28.7	35.9
Port Middle Nearshore	27.1	34.9	27.2	32.7	28.1	34.2	28.5	34.9
Port Middle Offshore	48.2	58.1	49.1	56.7	30.7	34.9	30.7	35.5
Port Northern Nearshore	25.6	27.96	25.9	28.2	36.2	40.6	36.3	42.1
Port Northern Offshore	24.6	28.5	25.5	28.7	29.4	35.7	29.4	36.6
Port Southern Nearshore	32.1	35.6	35.1	36	34.4	38.1	34.4	37.8
Port Southern Offshore	35.4	40.6	38.2	45.2	26.2	31.3	26.5	32.7
Preferential	47.9	52.9	52.4	56.2	32	36.1	37.8	37.4
Random	44.9	49.3	47.6	50.1	57.7	63.5	57.8	64.9

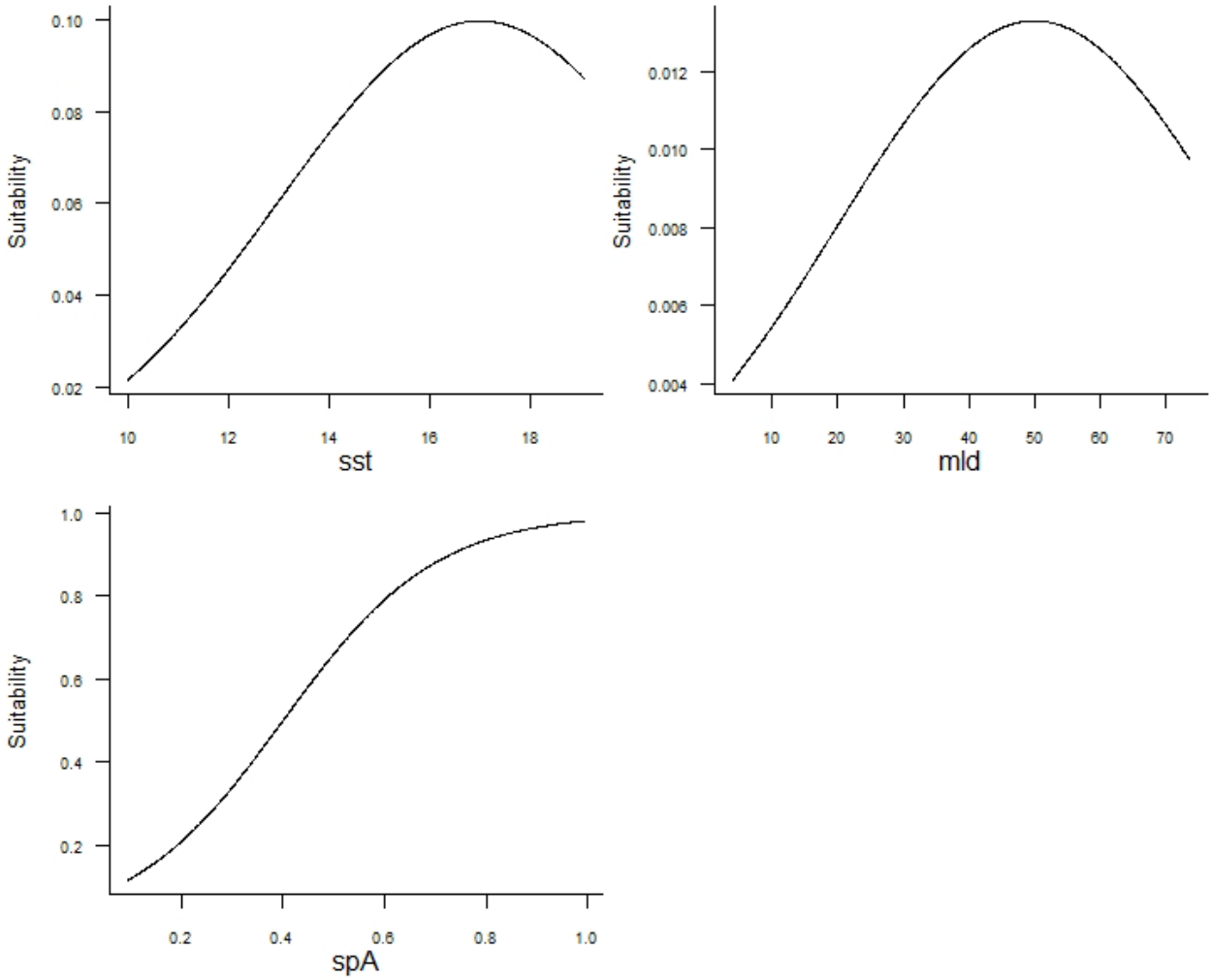

Figure S1. Virtual species response curves. ‘spA’ is the prey species, and represents the target species preference for its prey species.

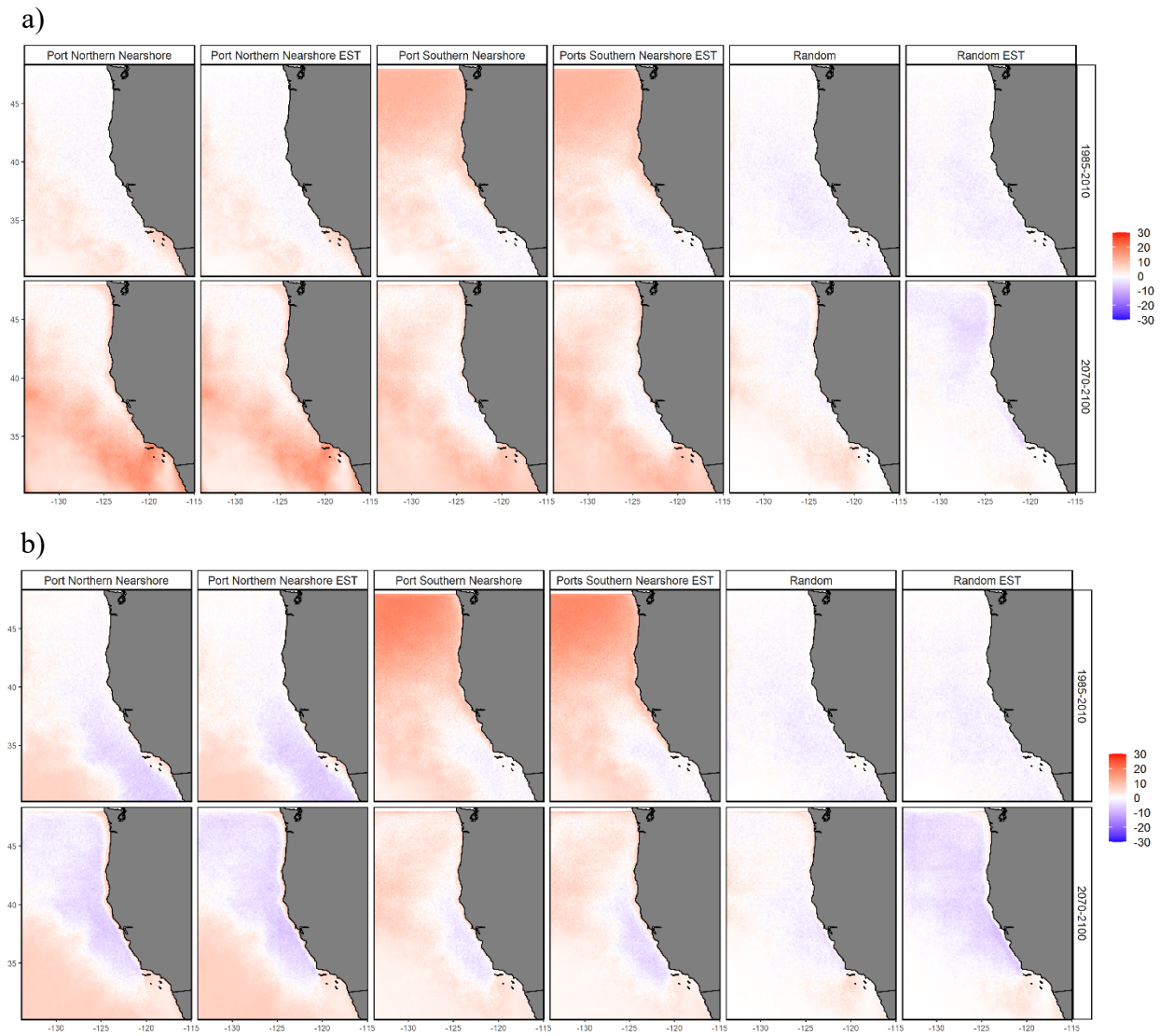

Figure S2: (a) Spatial residual (predicted – observed) maps for the GAM models, and (b) spatial residual maps for the BRT models for selected sampling scenarios fit Environmental covariates only, and Environmental and Space-Time covariates (EST). Only the historic training period (1985-2010) and late-century future period (2070-2100) are shown for simplicity.

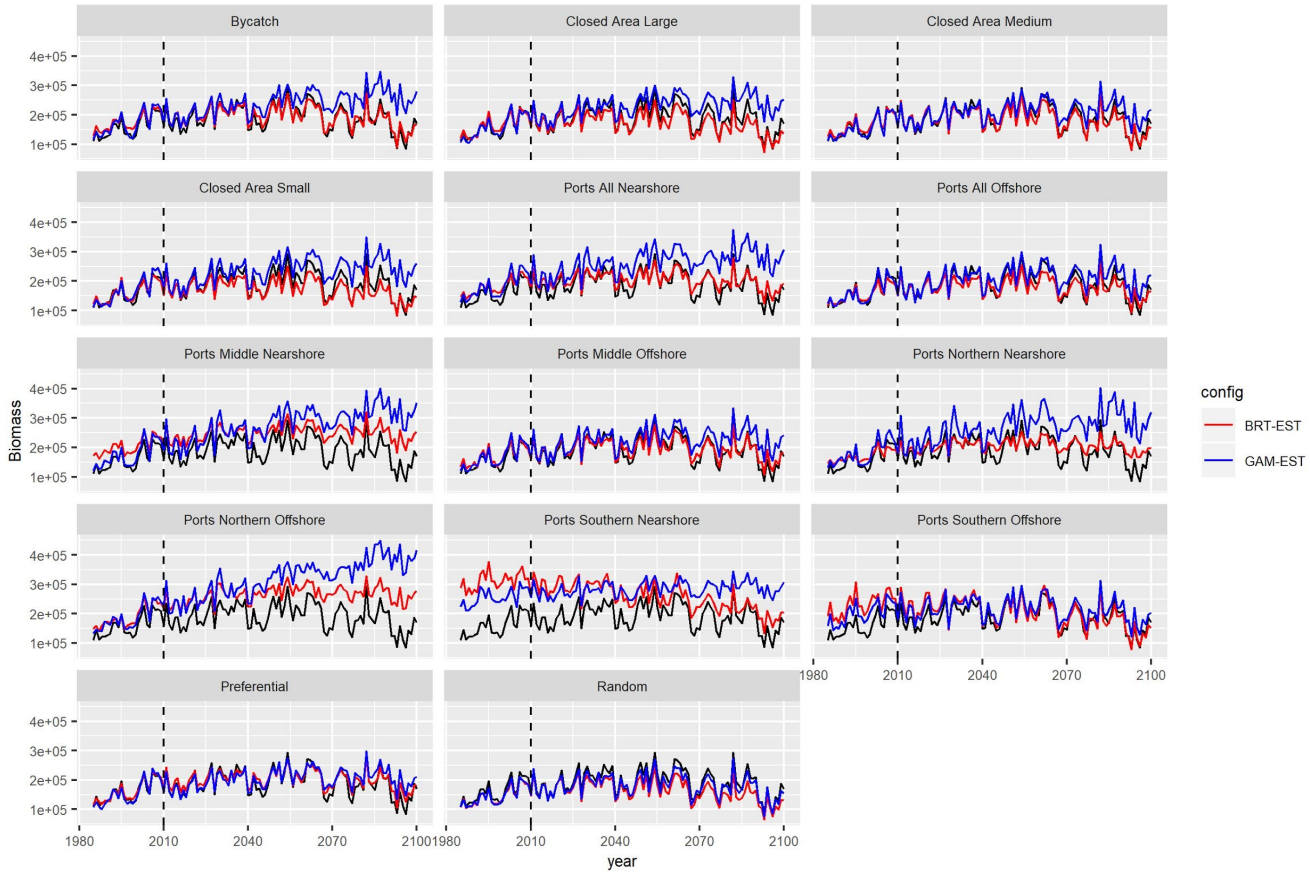

Figure S3: Biomass time series for models fit with space and time covariates as well as all three environmental covariates (MLD, SST, CHL).

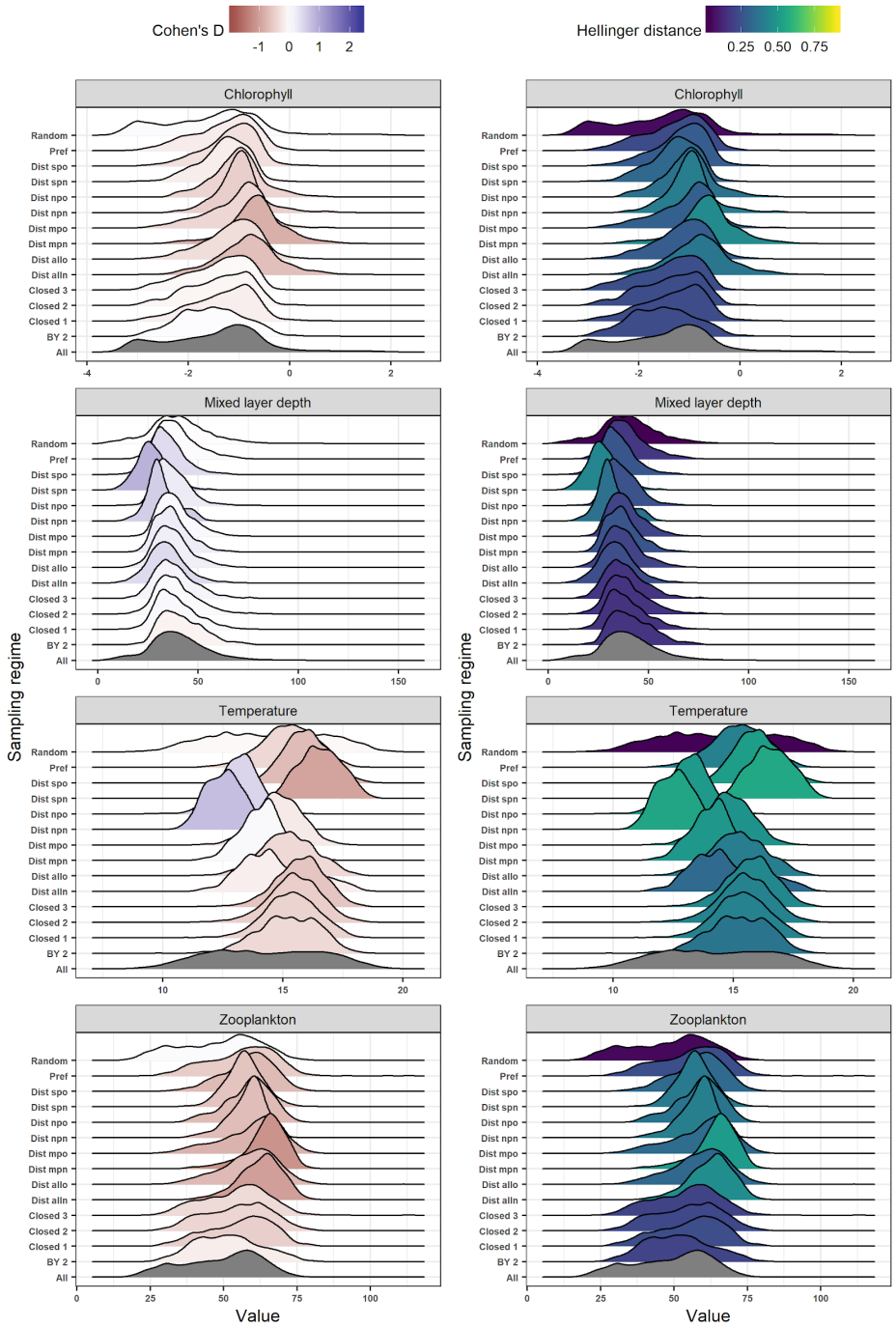

Figure S4: Distribution and climate bias of environmental variables in each sampling scenario for historical period (1985-2010). Colors indicate the magnitude of the climate bias of each sampling scenario, measured with Cohen's D (left panels) and Hellinger distance (right panels).

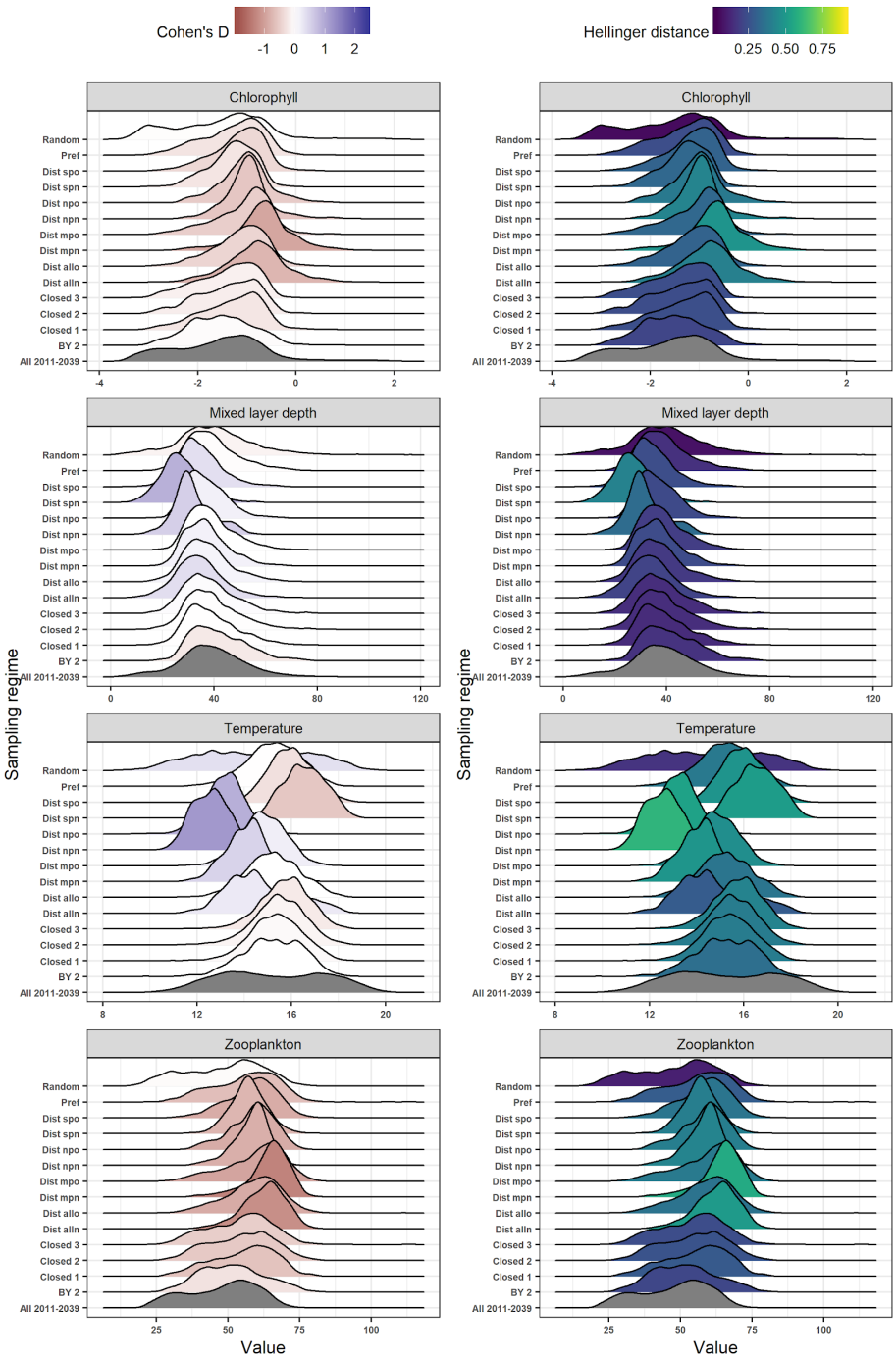

Figure S5: Distribution and climate bias of environmental variables in each sampling scenario for early-century period (2011-2039). Colors indicate the magnitude of the climate bias of each sampling scenario, measured with Cohen's D (left panels) and Hellinger distance (right panels).

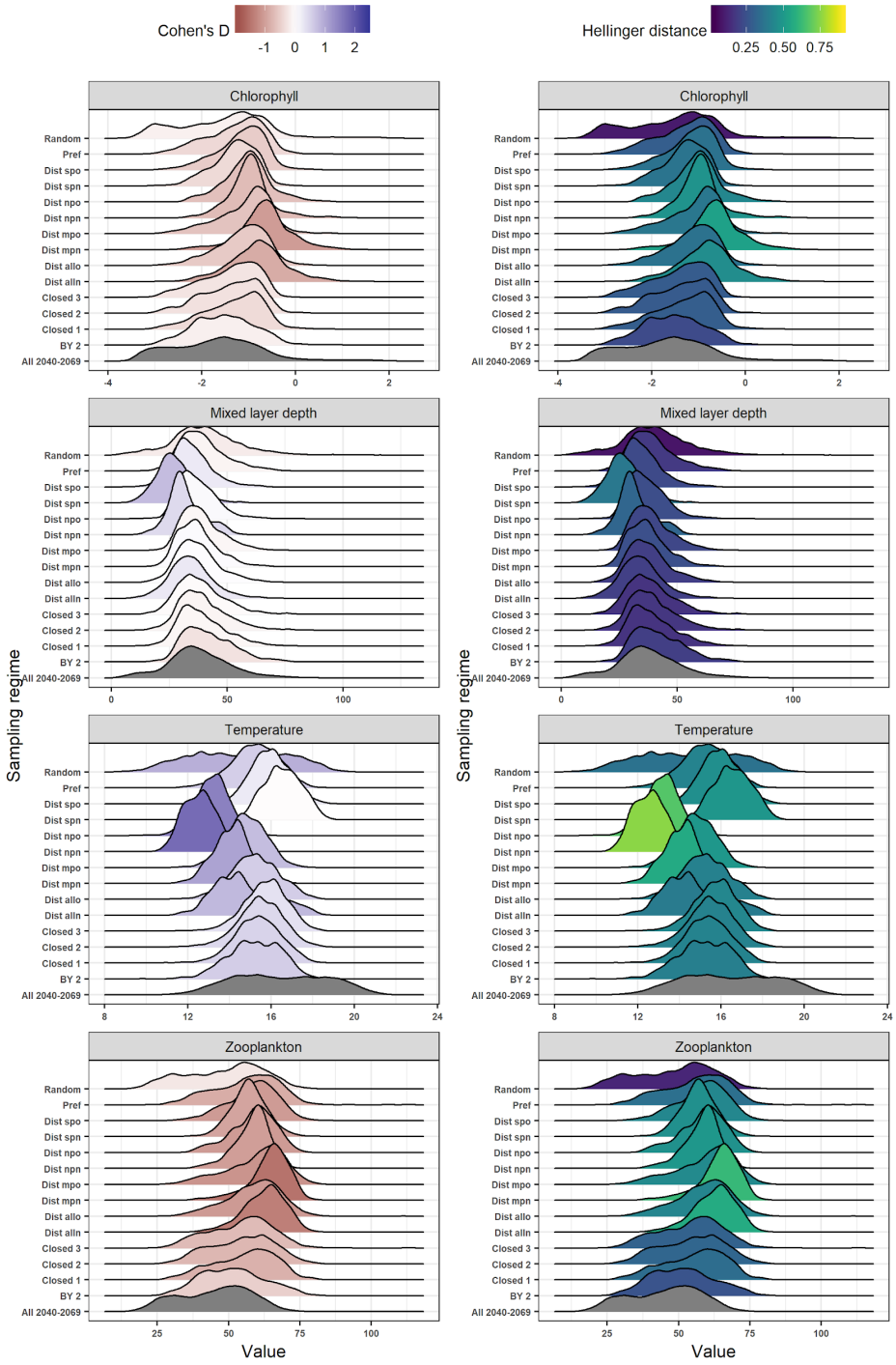

Fig S6: Distribution and climate bias of environmental variables in each sampling scenario for middle-century period (2040-2069). Colors indicate the magnitude of the climate bias of each sampling scenario, measured with Cohen's D (left panels) and Hellinger distance (right panels).

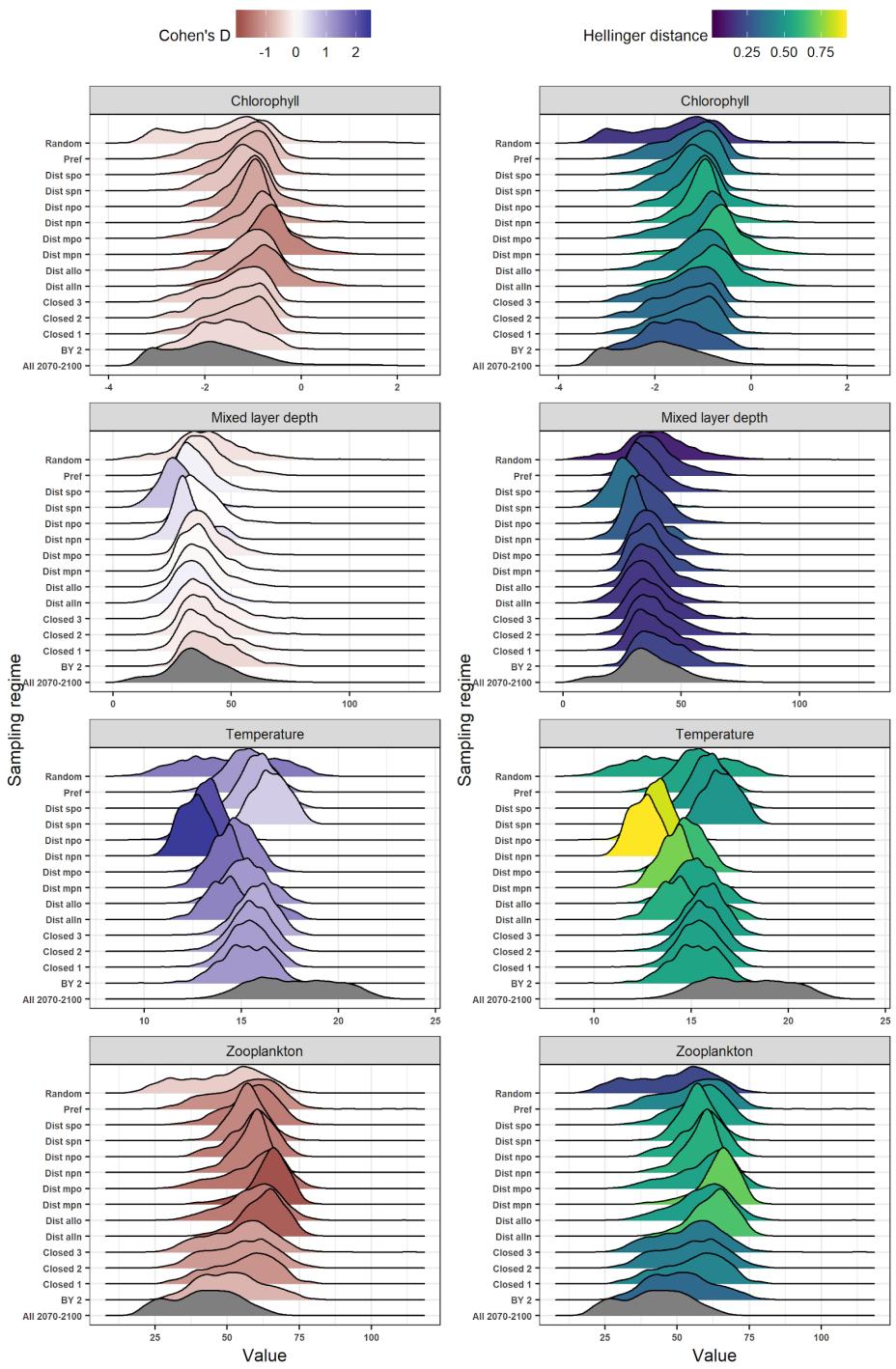

Fig S7: Distribution and climate bias of environmental variables in each sampling scenario for late-century period (2070-2100). Colors indicate the magnitude of the climate bias of each sampling scenario, measured with Cohen's D (left panels) and Hellinger distance (right panels).

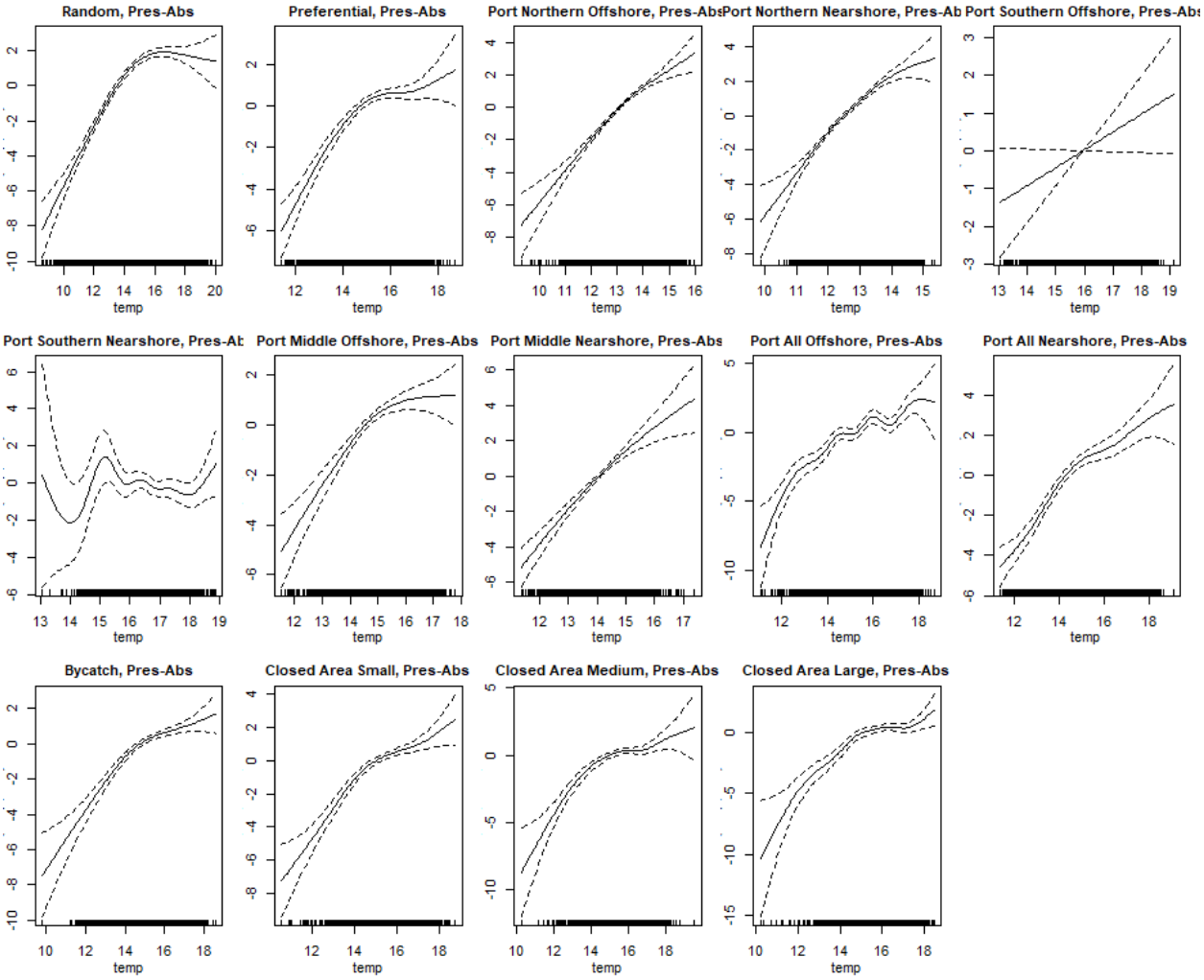

Figure S8. Sea surface temperature response curves for the binomial (occurrence, presence-absence) part of delta model (GAMs).

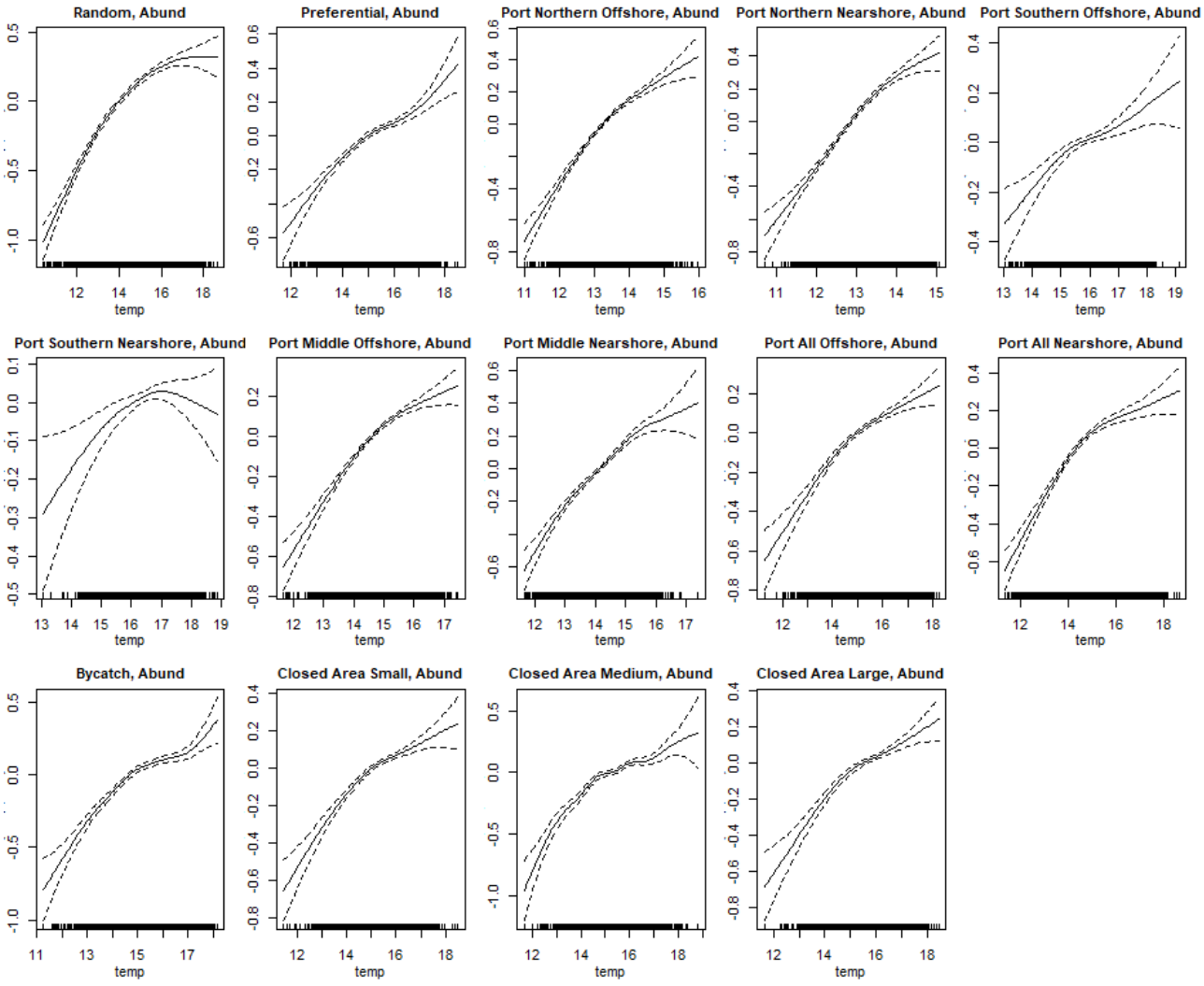

Figure S9. Sea surface temperature response curves for abundance part of delta model (GAMs).

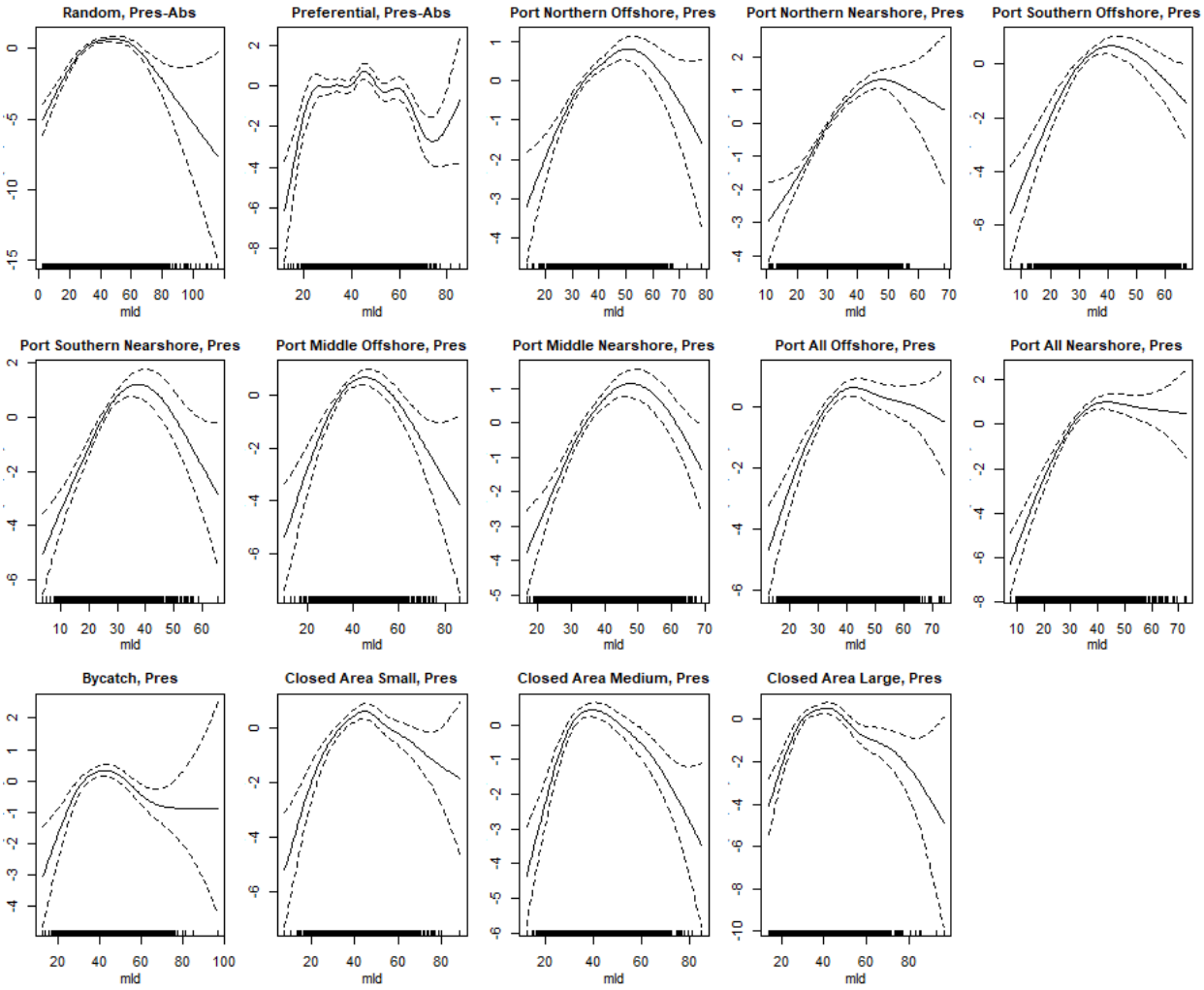

Figure S10. Mixed layer depth (mld) response curves for binomial (occurrence, presence-absence) part of delta model (GAMs).

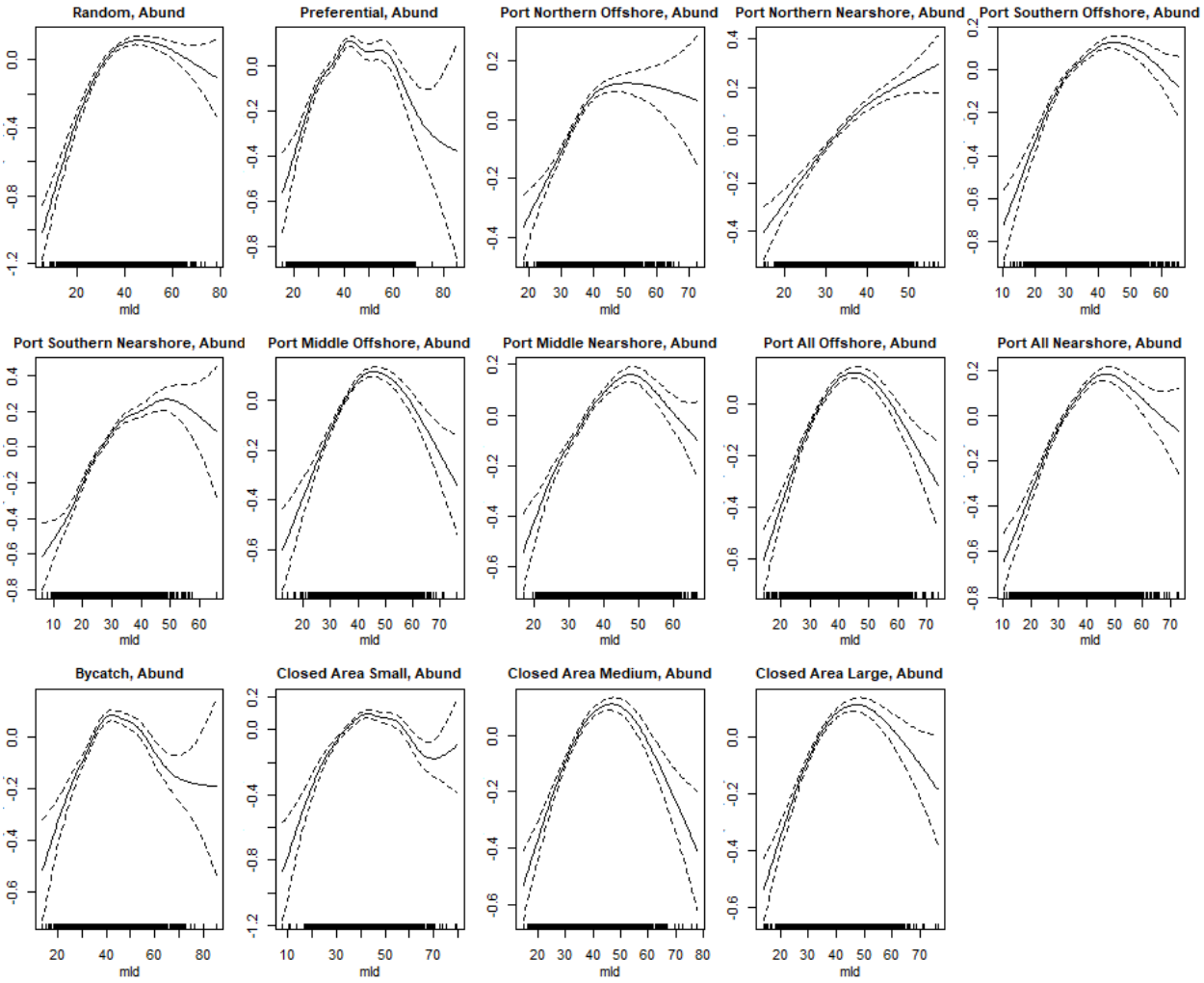

Figure S11. Mixed layer depth (mld) response curves for abundance part of delta model (GAMs).

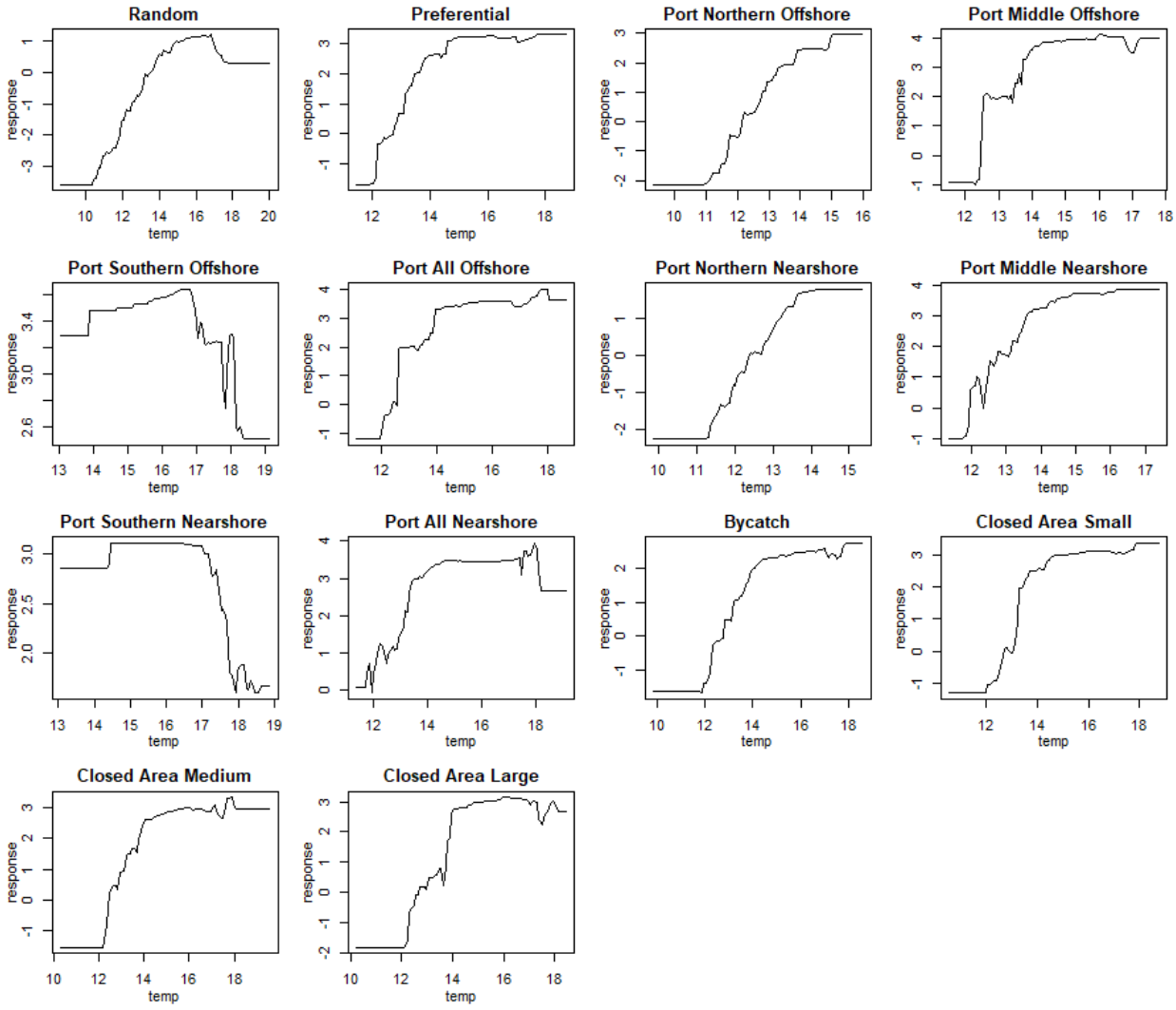

Figure S12. Sea surface temperature response curves for the binomial (occurrence, presence-absence) part of delta model (BRTs).

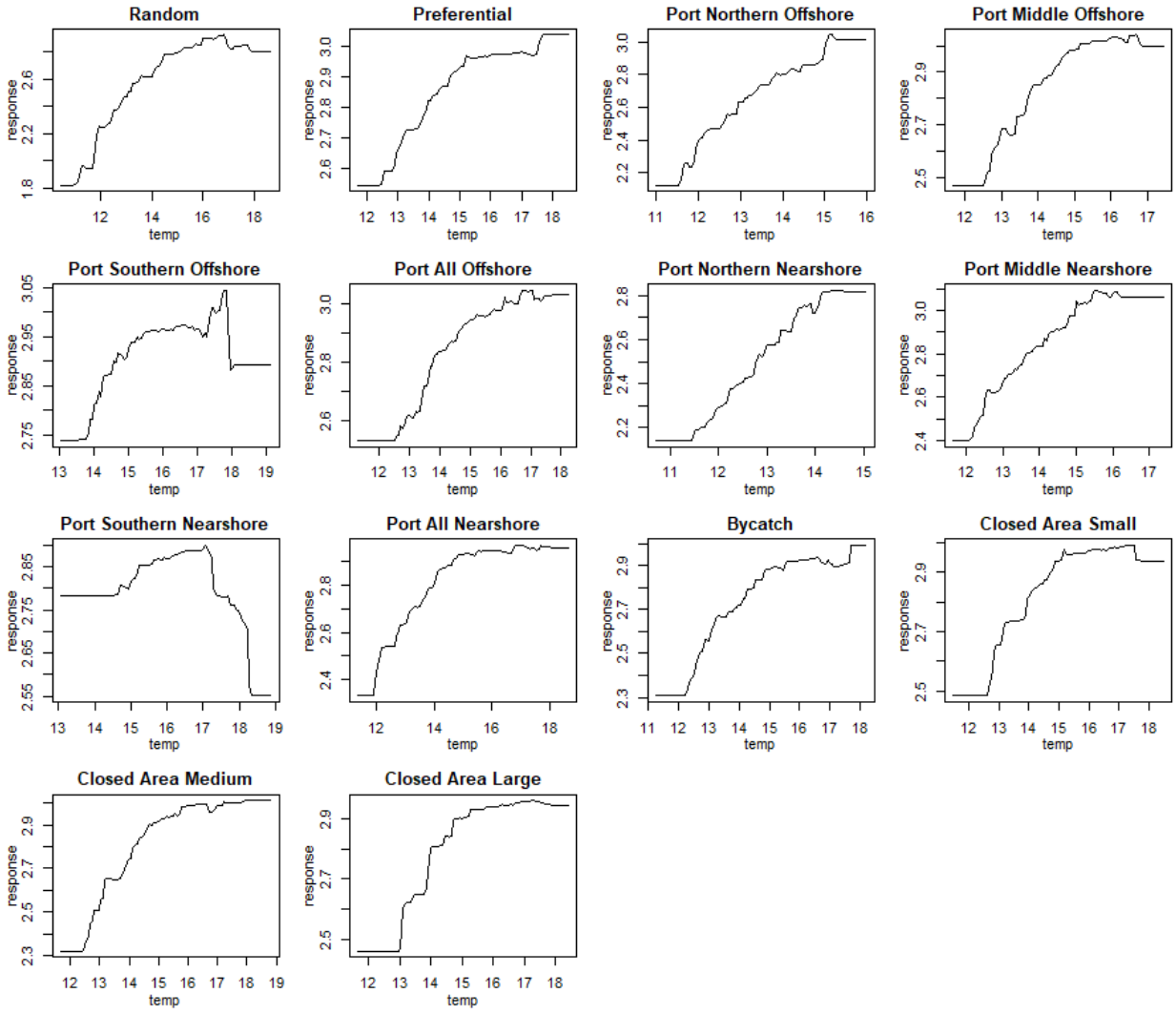

Figure S13. Sea surface temperature response curves for the abundance part of delta model (BRTs).

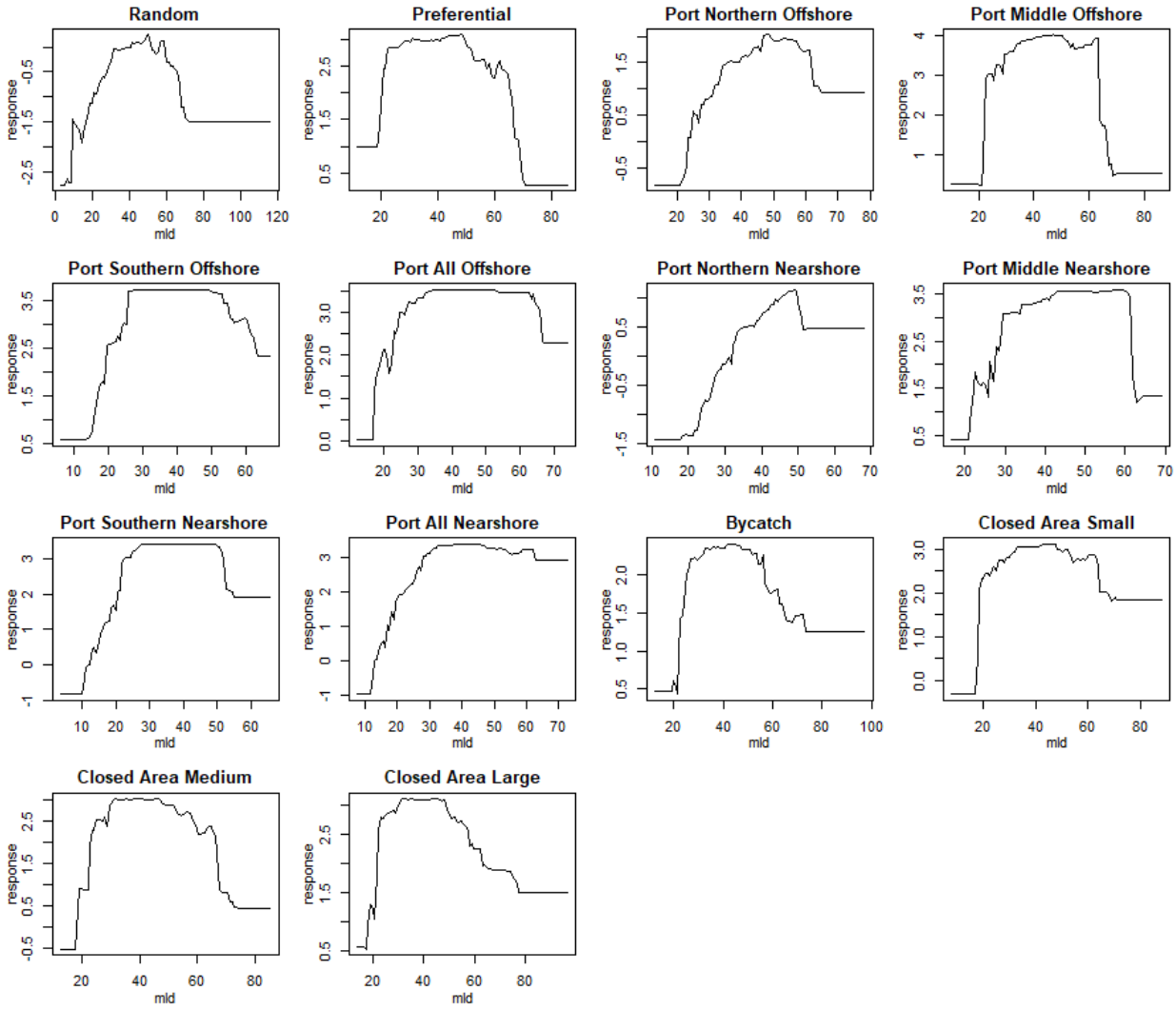

Figure S14. Mixed layer depth response curves for the binomial (occurrence, presence-absence) part of delta model (BRTs).

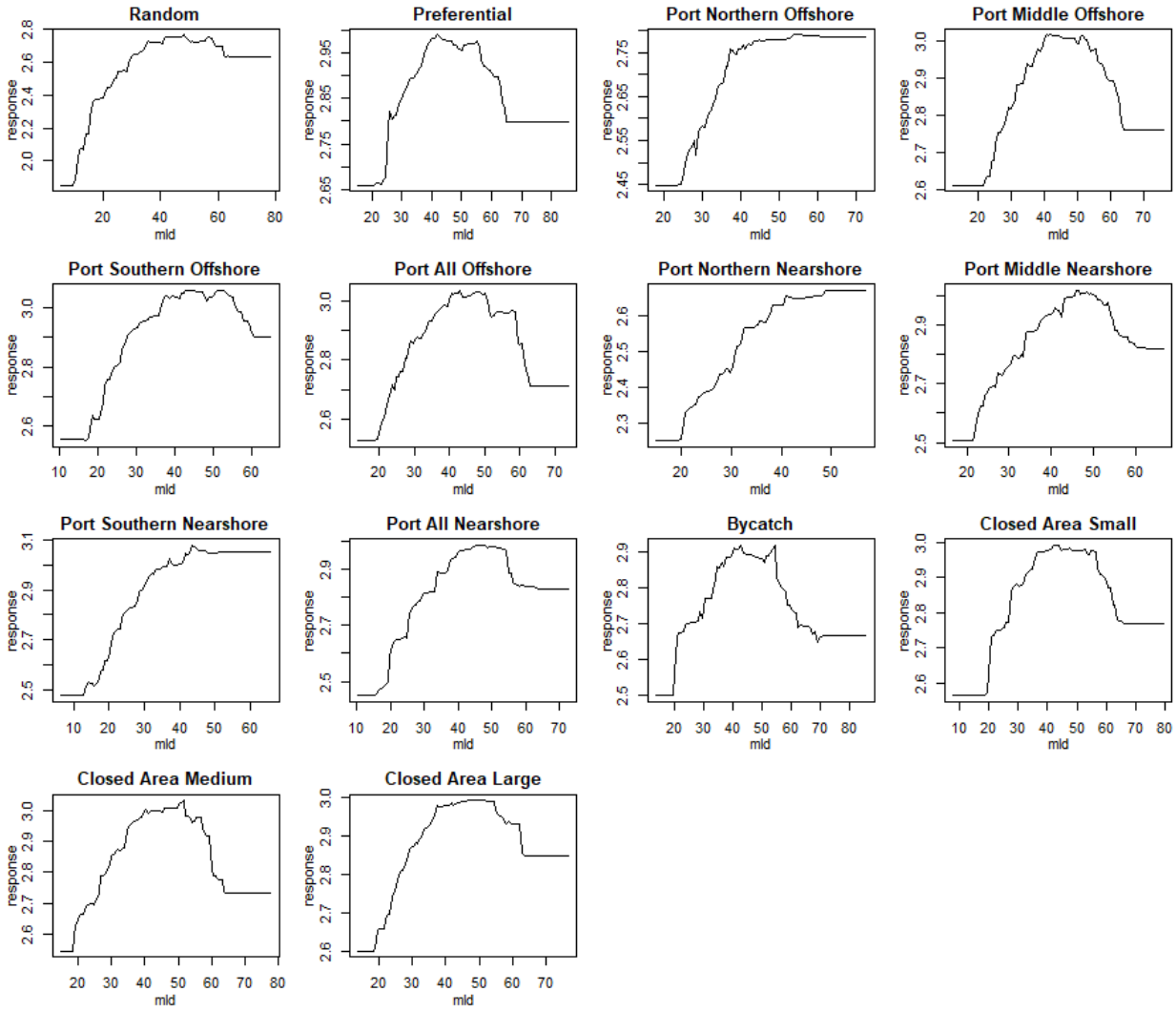

Figure S15. Mixed layer depth response curves for the abundance part of delta model (BRTs).

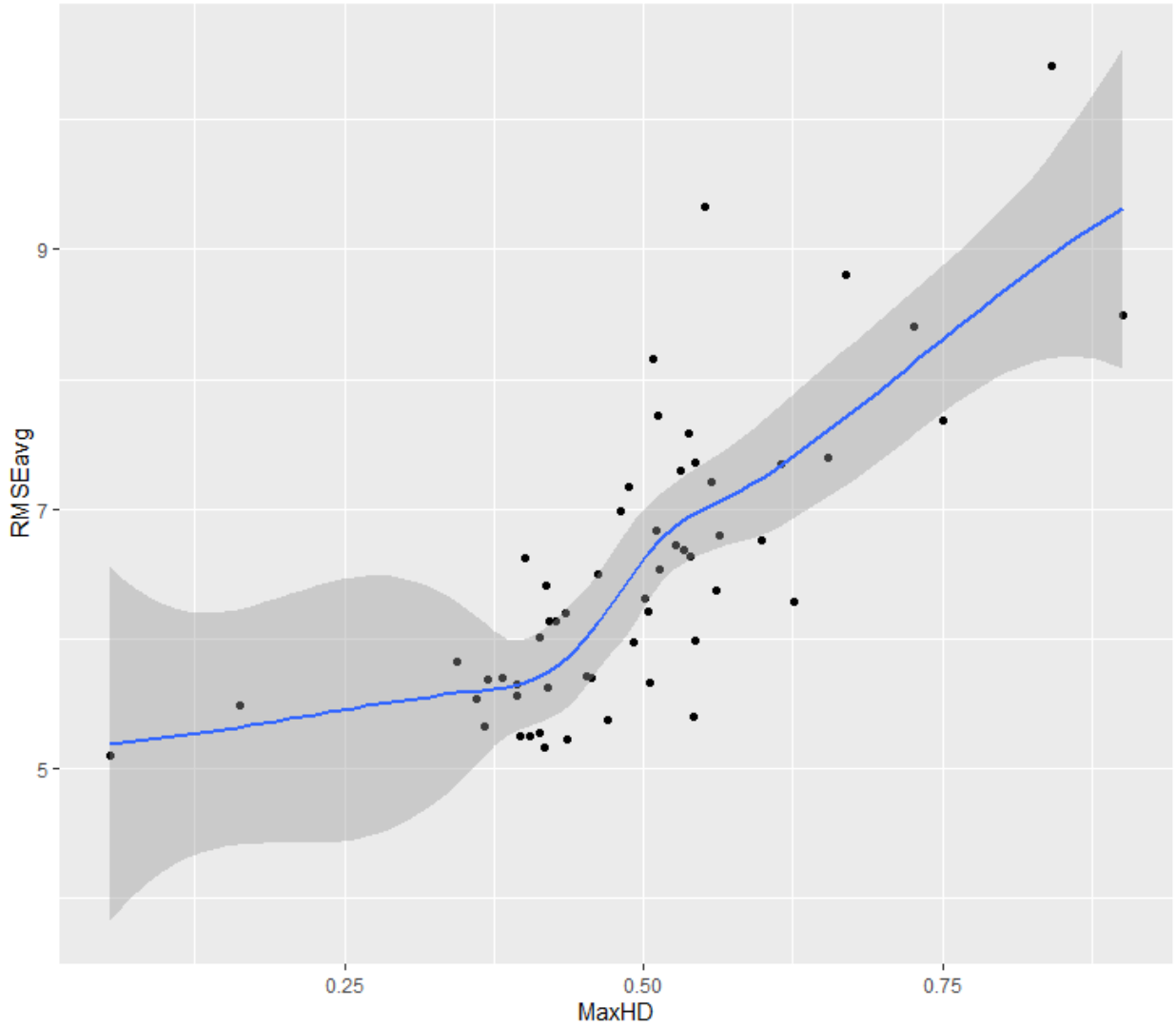

Fig S16: Comparison of Hellinger Distance (taken as the maximum HD across all climate variables for each sampling scenario and time period) and Mean RMSE.

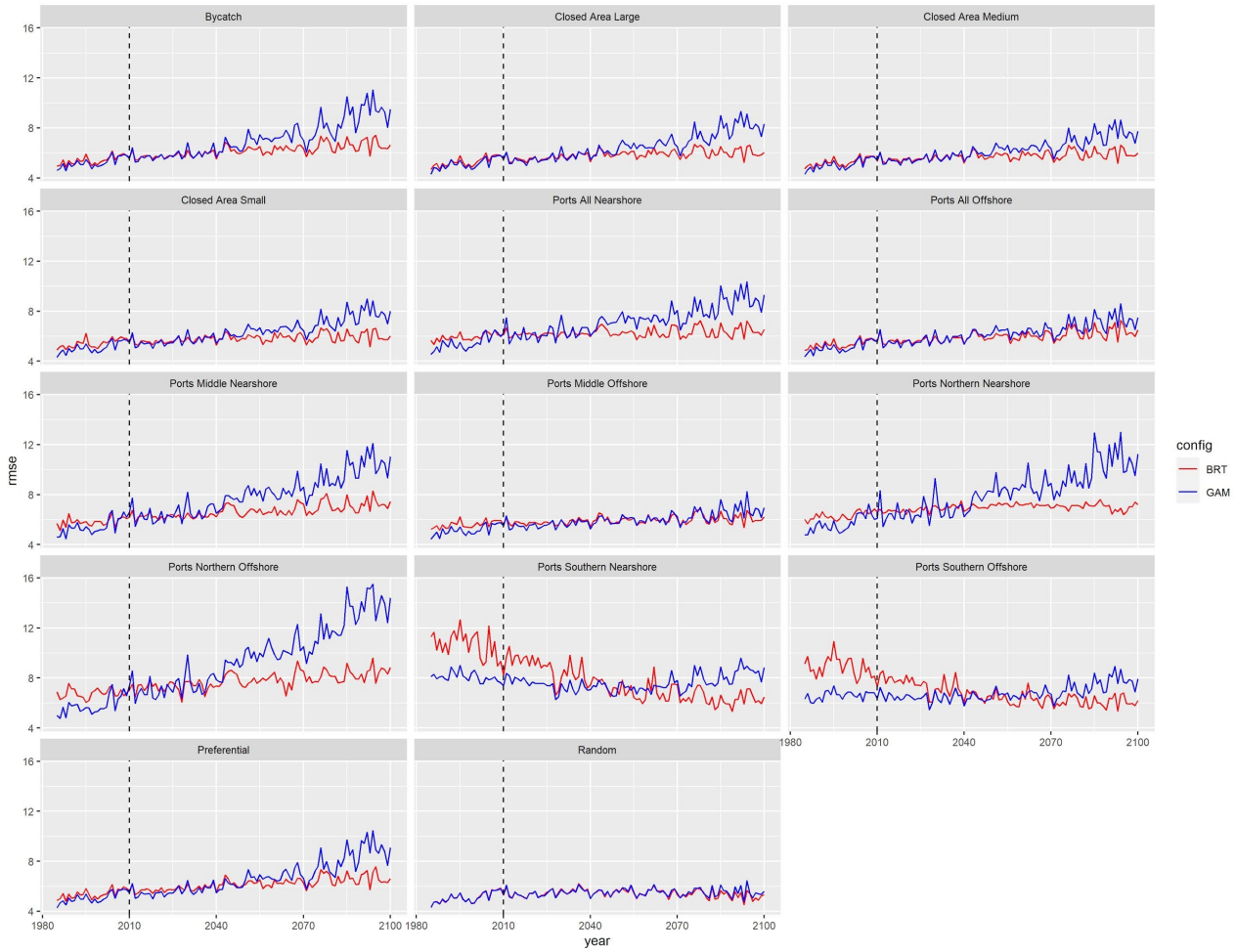

Figure S17: RMSE time series for models for 1985-2100. Each panel represents one of the 14 different fishing location scenarios, and each line represents the different model algorithm (GAM or BRT). Dashed line represents when the historical model fitting ends (1985-2010) and forecasts begin (2011-2100).

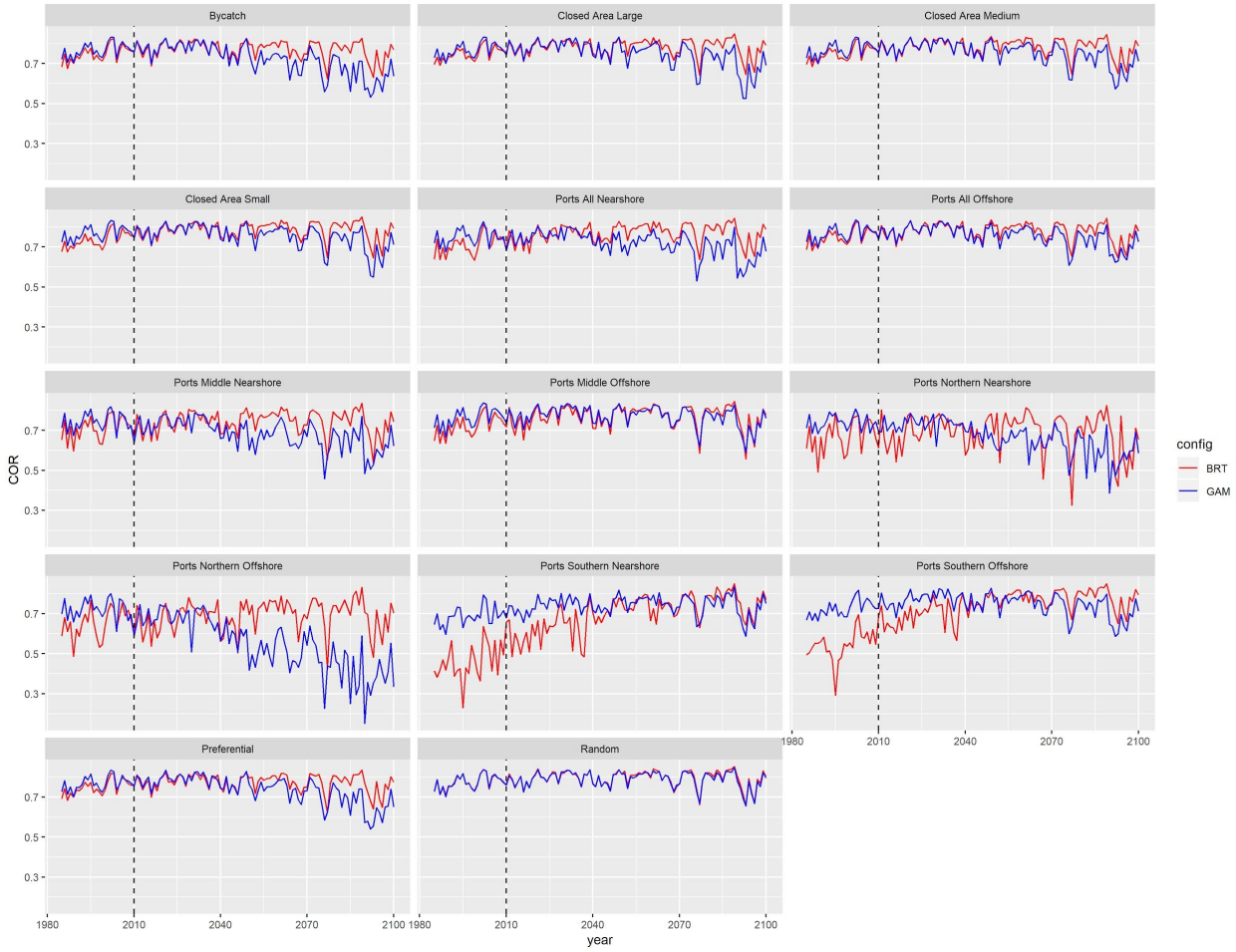

Figure S18: Time series of annually averaged correlation coefficients. Each panel represents one of the 14 different fishing location scenarios, and each line represents the different model algorithm (GAM or BRT). Dashed line represents when the historical model fitting ends (1985-2010) and forecasts begin (2011-2100).

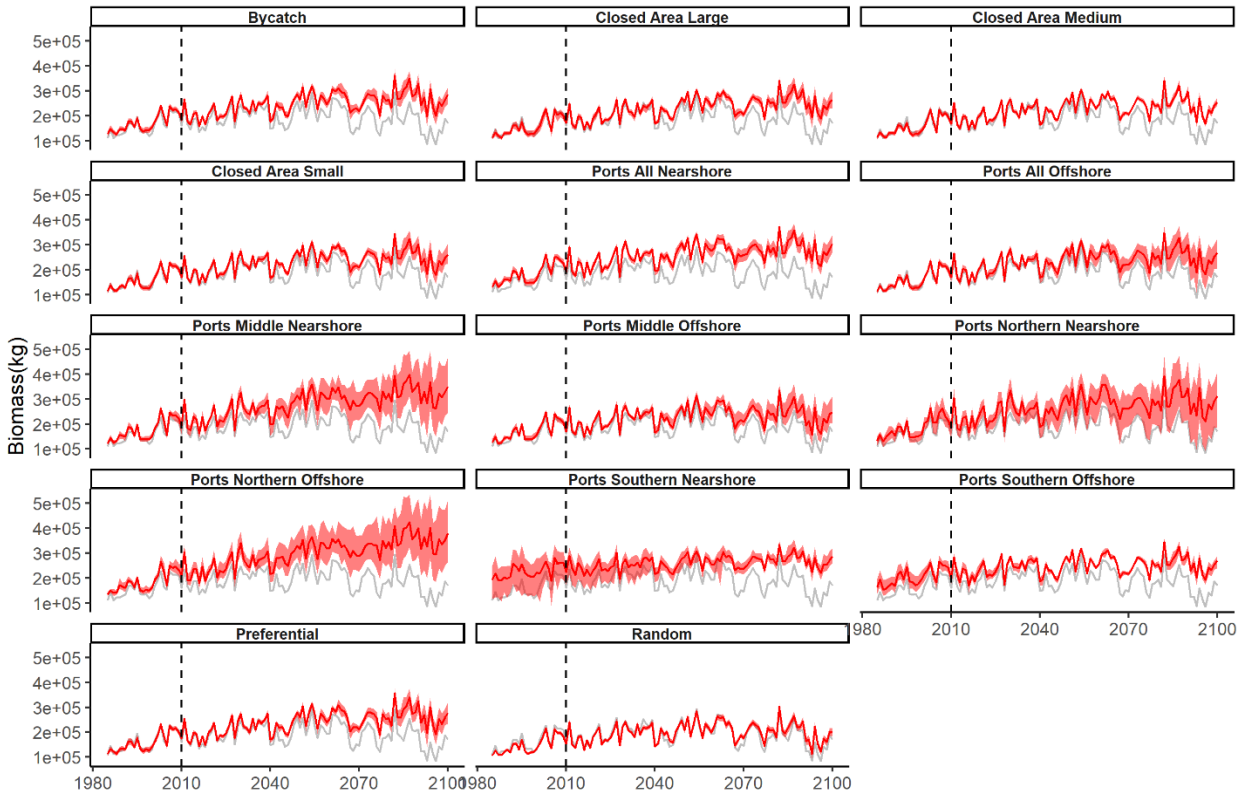

Figure S19: Time-series of simulated (grey line) and estimated (red line) biomass, with the within-model uncertainty for GAMs indicated by red shading. Results shown for each sampling scenario.

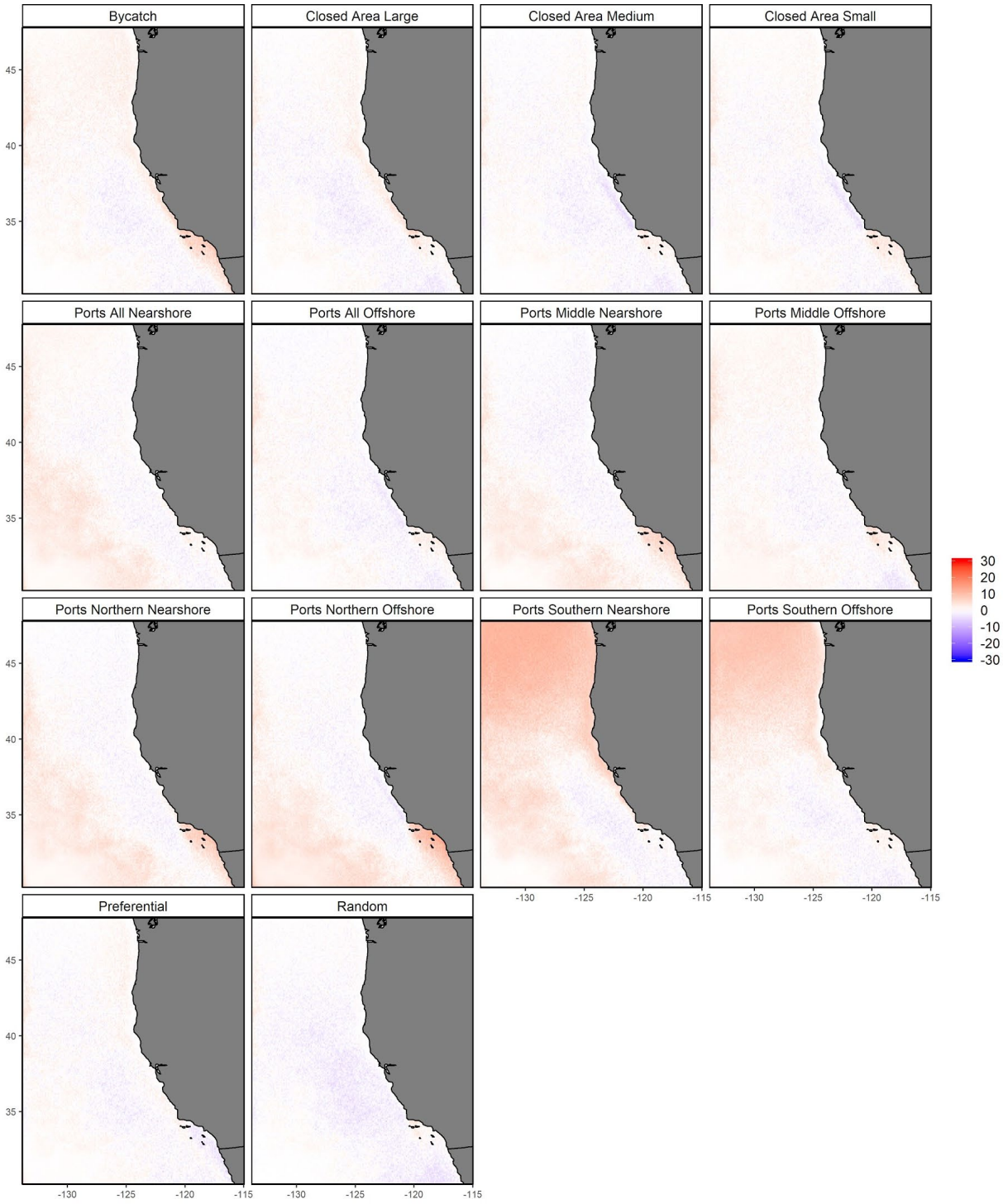

Figure S20: Difference between predicted and true abundance at each spatial grid cell for each sampling scenario for the historical (1985-2010) time period. Blue areas indicate areas where the model underpredicts the true abundance, and red areas represent the areas where the models overpredict the true abundance.

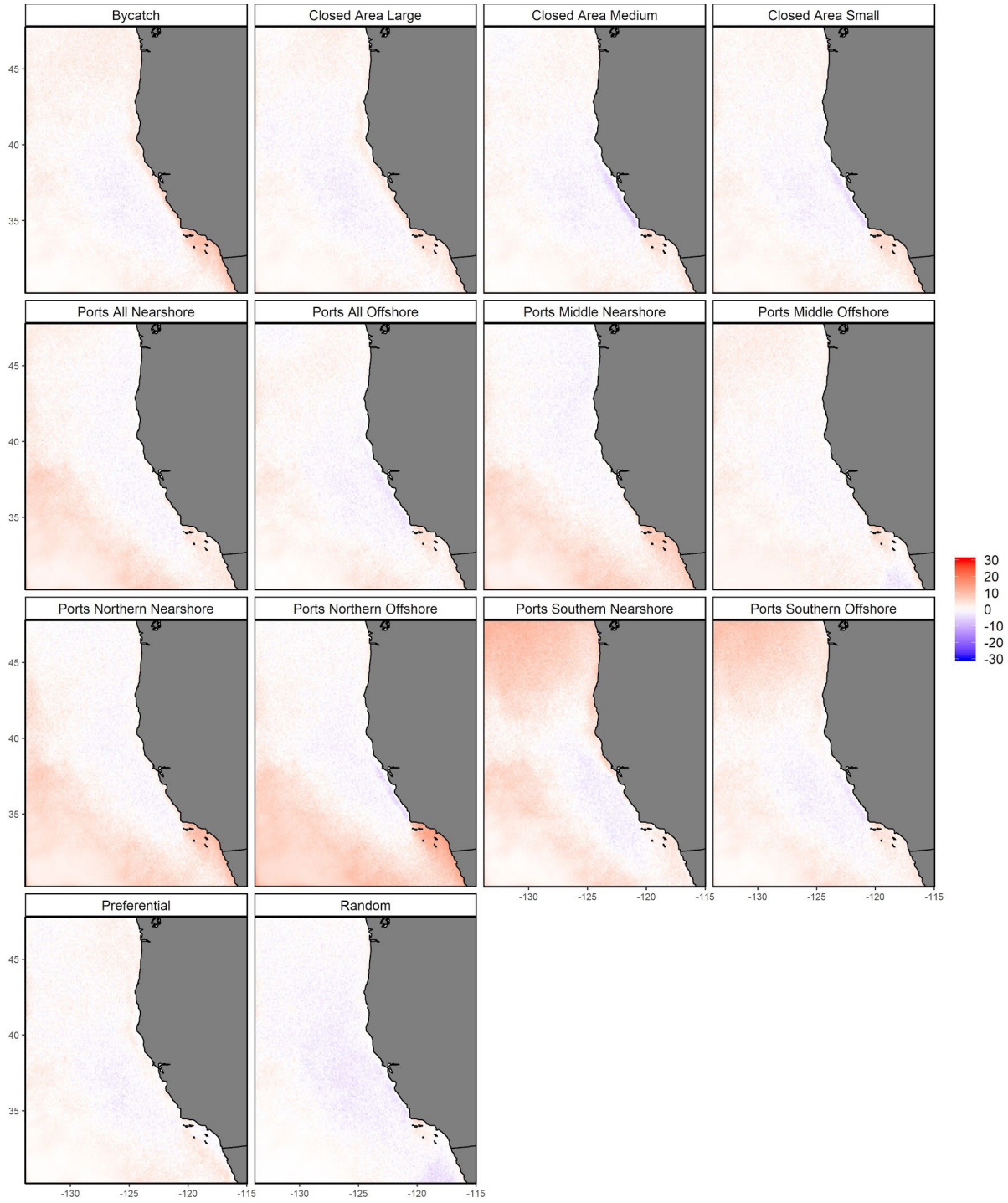

Figure S21: Difference between predicted and true abundance at each spatial grid cell for each sampling scenario for the early century (2011-2039) time period. Blue areas indicate areas where the model underpredicts the true abundance, and red areas represent the areas where the models overpredict the true abundance.

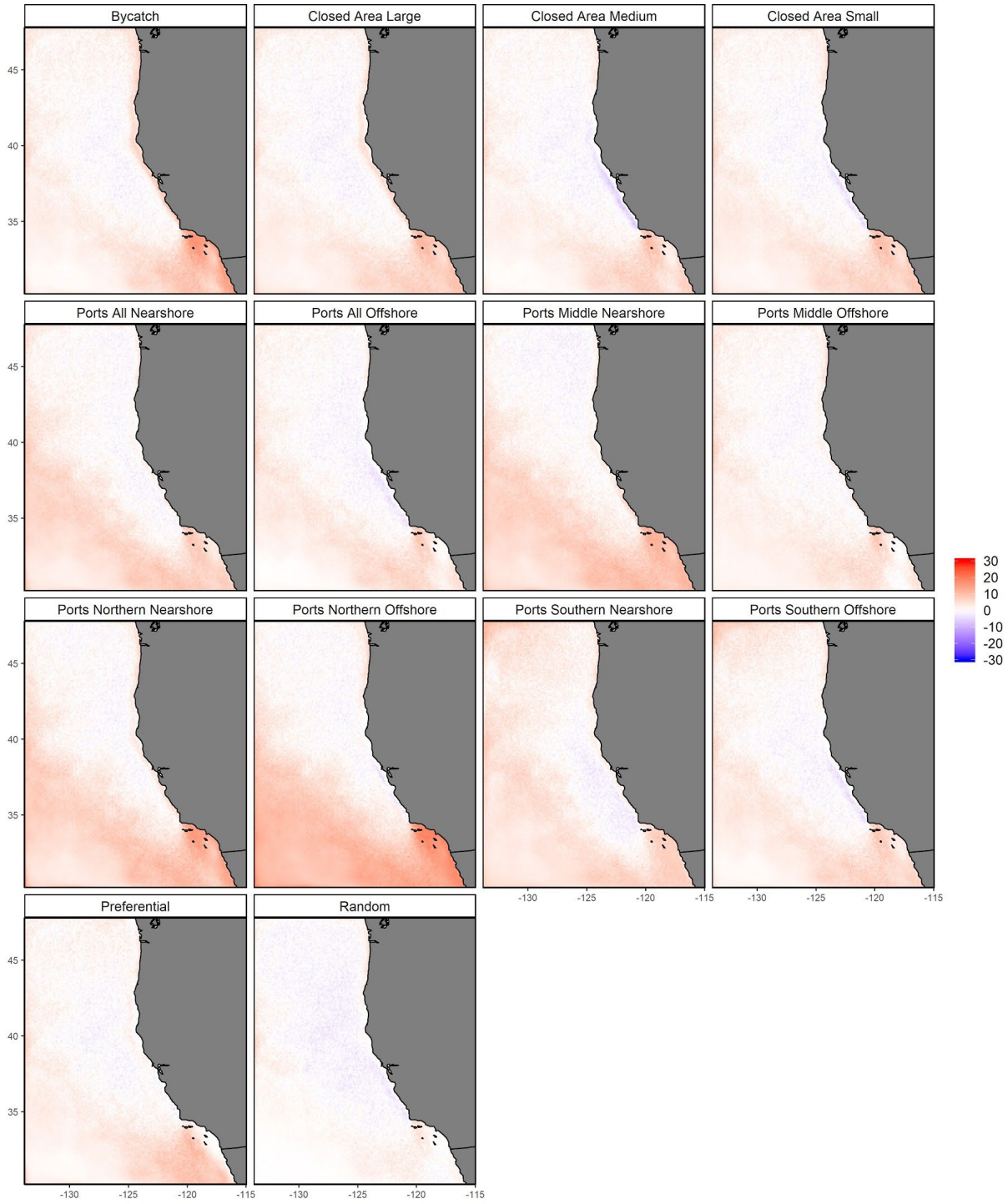

Figure S22: Difference between predicted and true abundance at each spatial grid cell for each sampling scenario for the mid-century (2040-2069) time period. Blue areas indicate areas where the model underpredicts the true abundance, and red areas represent the areas where the models overpredict the true abundance.

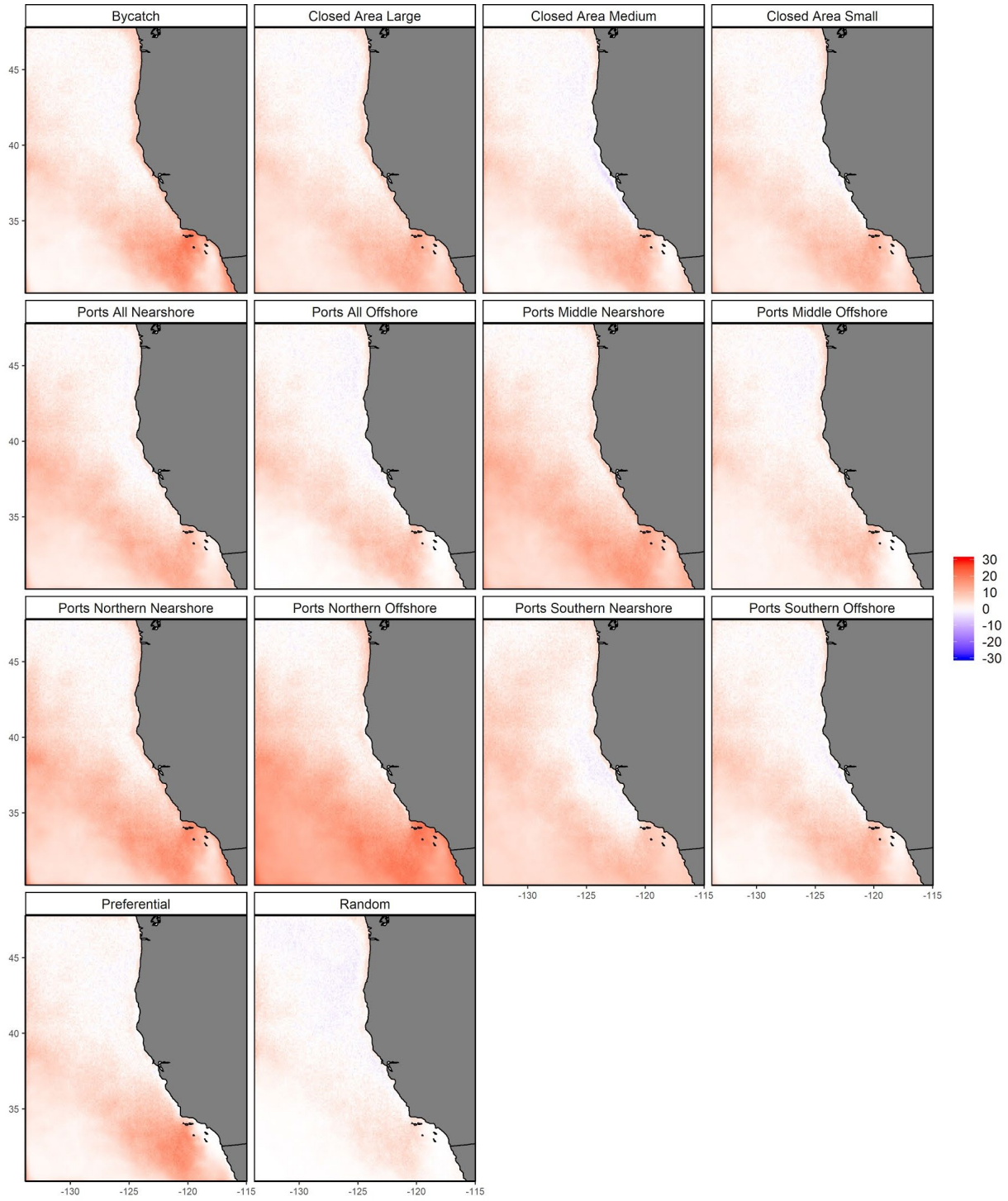

Figure S23: Difference between predicted and true abundance at each spatial grid cell for each sampling scenario for the late-century (2070-2100) time period. Blue areas indicate areas where the model underpredicts the true abundance, and red areas represent the areas where the models overpredict the true abundance.